agronomy

MDPI

Article

Genetic Analysis of Flowering Time of Ethiopian Barley Accessions Under Field and Climate Chamber Conditions

Surafel Shibru Teklemariam [1], Kefyalew Negisho Bayissa [2], Andrea Matros [3], Klaus Pillen [4], Frank Ordon [5] and Gwendolin Wehner [5,*]

[1] Melkassa Agricultural Research Center, Ethiopian Institute of Agricultural Research (EIAR), Melkassa P.O. Box 436, Ethiopia
[2] National Agricultural Biotechnology Research Center, Ethiopian Institute of Agricultural Research (EIAR), Holetta P.O. Box 249, Ethiopia
[3] COMPOLYTICS GmbH, Steinfeldstraße 3, 39179 Barleben, Germany; andrea.matros@compolytics.com
[4] Institute of Agricultural and Nutritional Sciences, Martin Luther University, 06120 Halle (Saale), Germany; klaus.pillen@landw.uni-halle.de
[5] Julius Kühn Institute (JKI), Federal Research Centre on Cultivated Plants, Institute for Resistance Research and Stress Tolerance, 06484 Quedlinburg, Germany; frank.ordon@julius-kuehn.de
* Correspondence: gwendolin.wehner@julius-kuehn.de

Abstract: The flowering time is one of the traits strongly influencing grain yield. In barley, the flowering time is mostly determined by the photoperiod, vernalization, and timely rainfall. As Ethiopia is located near the equator, the photoperiod and vernalization have a minimum effect on barley, but rainfall and temperatures are major challenges. In this study, 260 Ethiopian barley accessions were evaluated for flowering time at four different locations in Ethiopia in three years. Additionally, a set of 196 accessions was evaluated in climate chambers with corresponding environmental parameters. According to the results, the sum of the daily temperature of growing days strongly influenced the flowering time. The mean flowering time of the warmer Melkassa location was 15, 7, and 4 days earlier than of the cooler Holetta location and the less warm Debrezeit and Dera locations, respectively. On the other hand, the flowering time in the climate chamber was delayed by 52 and 37 days than that at the Melkassa and Holetta locations, respectively; its lowest average daily temperature (18 °C), compared to Melkassa (28.0 °C) and Holetta (22.1 °C), might be the reason. GWAS identified MTAs on chromosomes 5H at 571.62 to 572.54 Mb as strongly associated with the flowering time at warm locations (Melkassa, Dera, and Debrezeit); MTAs on chromosome 2H at 25.1 and 29.3 Mb turned out to be associated with the flowering time at Holetta and in the climate chamber, respectively. Important factors that influence the flowering times of Ethiopian barley landraces and associated SNP markers are identified in this study, which might be useful to consider in future barley breeding programs.

Keywords: barley; Ethiopian landraces; flowering time; growing degree days; temperature effect; GWAS

Citation: Teklemariam, S.S.; Bayissa, K.N.; Matros, A.; Pillen, K.; Ordon, F.; Wehner, G. Genetic Analysis of Flowering Time of Ethiopian Barley Accessions Under Field and Climate Chamber Conditions. *Agronomy* **2024**, *14*, 3031. https://doi.org/10.3390/agronomy14123031

Academic Editor: Andras Cseh

Received: 19 November 2024
Revised: 12 December 2024
Accepted: 17 December 2024
Published: 19 December 2024

1. Introduction

In Ethiopia, barley ranks fifth in terms of production area and total yield harvested; in 2018/19, 811,782.08 hectares of land were cultivated and an average of 2.18 tons per hectare was harvested, which accounts for 5.63% of the total cereal production [1]. It is the most adapted cereal crop, growing in a wide range of agro-ecologies, from low lands of drought-prone areas at 1500 m above sea level (masl) to the highlands of Ethiopia at 3400 masl [2]. The main purposes of barley are to prepare different types of food and local beverages [3].

Flowering is the most important stage in plant development, which significantly contributes to environmental adaptation and, ultimately, to grain yield [4,5]. Therefore, the complex trait flowering time is considered one of the key interventions in barley (*Hordeum vulgare* L.) breeding programs [6] and is of prime importance for improving yield and yield components [7,8].

Despite the fact that genes associated with barley's flowering pathways are not quite similar in the northern and south part of the hemispheres [9], it is difficult to pinpoint a gene that regulates flowering time, even in the northern hemisphere [10]. However, several studies identified genes associated with the length of photoperiod (*Ppd-H1* and *Ppd-H2*, which are located on chromosomes 2HS and 1HL, respectively), vernalization requirements (*Vrn-H1*, *Vrn-H2*, and *Vrn-H3* that are mapped on chromosomes 5HL, 4HL, and 7HS, respectively), and earliness per se (*ELF3*, *eps2S*, *sdw1*, *eps3L*, and *HvPHYC*, which are mapped on chromosomes 1H, 2H, 3H, 3H, and 5H, respectively); these are believed to be the most important genes [10–16].

The dominant *Ppd-H1* allele enhanced earlier flowering during the long photoperiod days than the recessive *ppd-H1* allele [15,17,18]. Because the dominant *Ppd-H2* allele is found in spring and winter barley genotypes, *Ppd-H2* is often described as a complex gene [15,19]; as a result, it is very difficult to categorize barley genotypes based on this flowering gene. *Vrn-H1* is the major regulatory gene for vernalization in barley [20]. The winter genotypes with the *vrn-H1* allele require prolonged exposure to cold temperatures in order to complete the transition from the vegetative stage to the flowering development stage in a timely way [15,21]. On the other hand, the deletion or insertion in the first intron of the *Vrn-H1* gene significantly affects the length of cold exposure [10,17,22], which benefited the wide adaptation of barley to different environments [23,24]. Winter barley types have the dominant *Vrn-H2* allele, which has a high expression during the winter period, which helps to enhance flower induction [21].

Although the importance of environmental cues like day length (photoperiod) and an extended exposure to cold temperature (vernalization) are described to determine the flowering time in barley, these factors may not be important for Ethiopian barley landraces. Being located near the equator (between 3.3° and 14.9° N of the latitude), there is an insignificant difference between the day and night length throughout the year and there is no cold winter. Rather, thermal time (growing degree-days (GDD) [°C d]) may influence the optimal time of flowering in Ethiopian barleys [25–27]. GDD is calculated as the sum of the temperatures required to reach a certain developmental stage [28,29]. A range from 756 to 1382 GDD from seedling emergence to the heading of barley was reported by Juskiw et al. [30], and, Ibrahim et al. [31], while the GDD for anthesis was reported in a range from 705 to 966 by Juskiw et al. [30].

Although Ethiopian barley landraces are characterized as spring types [32], a low frequency of lines respond to minimal vernalization temperatures (<4 °C), as previously observed by Knüpffer et al. [33]. In the Tibetan plateau, over 4000 masl, the winter varieties of barley grew very well, despite the dominance of spring varieties in this region [33,34]. As a result, the requirement of the low vernalization of few Ethiopian landraces may be related to the adaptation of landraces at extremely high altitudes in Ethiopia. According to Tsehaye et al. [35], Ethiopian landraces also exhibit strong responses to long days, and flower as early as 4–5 weeks after sowing.

Tsehaye et al. [35] reported that Ethiopian landraces possess the *Ppd-H2* allele, which responds to short photoperiods (SD), also known as "non-inductive SD conditions". This allele utilized the GA pathway to induce flowering under SD conditions, in which the flowering time is controlled by *SOC1* (*SUPRESSOR OF OVEREXPRESSION OF CO 1*) and *LFY* (*LEAFY*) genes [11]. The presence of the *Ppd-H2* allele in barley could also be related to the requirement for milder winter temperatures, which was reported for Mediterranean barley genotypes [19]. Tsehaye et al. [35] also detected QTLs related to *HvFT4* (57.9 Mb) on chromosome 2H, *HvFT2* (101.6 Mb) on chromosome 3H, *HvFT5* (609.4 Mb) on chromosome 4H, *HvCO3* (358.1 Mb) on chromosome 5H, *HvCO2* (488.4 Mb) and *HvCO5* (357.5 Mb) on chromosome 6H, as well as *HvCO8* (50.1 Mb) in proximity to *HvCO1* (*Vrn-H3*) on chromosome 7H, which are mapped based on the Morex genome v2 reference [36]. Caproni et al. [37] also reported that the flowering of Ethiopian landraces is associated with the *Vrn-H1* and *FRIGIDA* of chromosome 5H. It has been documented that *FRIGIDA*, also known

as *FRI*, influences the adaptation of *Arabidopsis* during high temperatures and drought stress [38].

Hemming et al. [39] reported that Ethiopian barley landraces carry *HvVRN1-1*, *HvVRN1-2*, *HvVRN1-4*, *HvVRN1-5*, and *HvVRN1-8*, which have different deletions in intron-I of the *HvVRN1* allele. Of these types, only lines carrying the *HvVRN1-1* allele type are reported to take longer than 100 days (d) from sowing to flowering, whereas all other types were reported to flower in less than 60 d in Mediterranean conditions. Wang et al. [40] reviewed that a mutation in the promoter region of *HvVRN1* or a deletion in the first intron are responsible for the reduced requirement of vernalization.

The drought stress experimental sites used in the studies of Teklemariam et al. [41] had a higher minimum and maximum temperature compared with optimal moisture sites. This resulted in an accelerated flowering time at the drought stress locations by 10% compared to naturally optimal moisture locations. Similarly, in that study, the flowering time in climate chamber experiments was delayed by 39 and 46 d compared to naturally optimal moisture and drought stress treatments in field experiments, respectively [41]. These results highlighted the diversity of the set of 260 Ethiopian landrace accessions regarding flowering time and their potential for further genomic analysis for this trait.

Therefore, this study is focused on exploring environmental factors associated with flowering time as well as the identification of marker trait associations (MTAs) in the barley genome that influence the flowering time of Ethiopian barley in different agro-ecologies as well as in controlled climate chamber conditions, using genome wide association studies (GWAS).

2. Material and Methods

2.1. Experiment Setup

The experiments were conducted during the major growing season in Ethiopia (June–September), at four locations, i.e., Holetta, Debrezeit, Melkassa, and Dera for three years (2016–2018), hereafter named as HL, DZ, MK, and DR, respectively. Due to a poor stand in DZ during 2018, these data were omitted from further analysis.

The climate chamber experiment was conducted in 2018 at the Julius Kühn Institute (JKI), Federal Research Centre for Cultivated Plants, Institute for Resistance Research and Stress Tolerance, Quedlinburg, Germany, which will be designated as CC in this study. The altitude, seasonal temperature, rainfall, and soil characteristics of the field research sites are described in Table 1.

A total of 260 barley accessions were included in the field experiments, of which 239 accessions were provided by the Ethiopian Biodiversity Institute and 21 barley breeding lines were provided by the Holetta National Barley Improvement Program. Detailed information about the plant material is presented in Teklemariam et al. [42]. The accessions were evaluated using an alpha-lattice design comprising three replications. Each replication comprised 20 incomplete blocks of 13 experimental plots, as described in Teklemariam et al. [41].

For the CC, a set of 196 accessions was selected. Pots with a size of $15 \times 15 \times 20$ cm^3 were filled with 1500 g of substrate (Einheitserde ED73, H. Nitsch & Sohn GmbH & Co. KG, Kreuztal, Germany). In each pot, three plants were grown. The experiment was performed using a complete randomized design with four replications. All pots were watered up to 70% of the soil water capacity (WC), as described in Teklemariam et al. [41]. A photoperiod of 13/11 h day/night was applied; the temperature of the climate chamber was 18/14 °C day/night during vegetative growth and increased to 22/16 °C when five to ten pots started to flower.

Table 1. Summary of seasonal weather, altitude, and soil characteristics of experimental locations during the experimental period (2016–2018).

Characteristics	Holetta	Debrezeit	Melkassa	Dera
Altitude (masl)	2400	1900	1550	1620
Maximum temperature (°C) *	21.7	25.3	28.2	26.2
Minimum temperature (°C) *	8.7	12.5	15.1	14.9
Rainfall (mm) *	732.4	470.3	546.7	381.6
Soil type	Nitosol	Vertisol	Hypo Calcic andosol/fulvisols	Calcic fulvic regosol
Soil texture	Clay	Clay	Clay loam to Clay	Clay loam
Soil pH (H_2O method)	5.48–5.90	6.23–7.14	7.22–7.55	7.04–8.10
Organic matter (%)	2.03–4.41	1.26–2.63	1.78–3.14	2.08–3.95
Cation exchange capacity (cmol/100 g)	19.11–33.18	35.19–48.15	21.63–32.28	27.30–37.17
Exchangeable sodium (%)	0.01–0.46	0.01–0.48	0.02–1.47	0.02–0.57
Bulk density (g/cm^3)	1.12–1.37	1.15–1.45	1.1–1.34	1.29–1.34

* The cropping season was from June to September for Holetta and from July to September for others.

2.2. Data Collection

In the field, each experimental plot was evaluated for days to flowering (DFL), i.e., when approximately 50% of the main inflorescence emergence was completed in Zadoks' stages 58 (Z58). In the CC, due to some accessions being unable to fully complete ear emergence, the time when 50% of the main spike awn was visible in Zadoks' stages 49 (Z49) was considered as DFL [43].

A few accessions did not flower during the experimental period in certain locations and CC. Therefore, days to reverse flowering (DRFL) was considered for data analysis. DRFL was calculated by subtracting the last maturity date of an experimental plot at a specific location from the flowering date. Accessions which did not flower during the experimental period have "0" values, whereas early flowering accessions have the maximum value for DRFL. To calculate DRFL, the maximum growing days of 155, 136, 123, 124, and 232 were used for HL, DZ, MK, DR, and CC respectively.

Metrological data, including daily minimum and maximum temperature and daily total rainfall, were recorded for each location from the first day of sowing to the maturity of the last plot. The cardinal temperatures, which consist of base temperature (T_b), optimal temperature (T_o), and ceiling temperature (T_c) were used to analyze the optimal growth as well as chilling requirements of Ethiopian landrace accessions. T_b, T_o, and T_c cardinal temperatures for optimal barley growth have been reported to be 0 °C, 21–28 °C, and 35 °C, respectively [44–46]. According to Chujo [47], cited in Porter and Gawith [48]), an optimal chilling temperature (T_{oc}) of 3.8–6.0 °C, base chilling temperature (T_{bc}) of −1.3 °C, and ceiling chilling temperature (T_{cc}) of 15.7 °C were reported.

When the daily maximum temperature was between T_b and T_o, the day was considered optimal for barley growth; however, when it was below T_b or exceeded T_c, the day was considered suboptimal for barley growth, further plant development halted, or the plant died. The daily chilling temperature requirement was met when the daily minimum temperature was between T_{bc} and T_{oc}; when the daily minimum temperature was higher than T_{cc} or lower than T_{bc}, the chilling temperature requirement was deemed unmet, and accessions that required vernalization delayed or failed to flower in a timely way.

Based on each day's maximum and minimum temperature, the proportion of optimal growing days [44–46] and days that met the chilling temperature requirement [47] was calculated.

Usually, growing degree days (GDDs) (in °C d) are calculated based on the daily mean temperature when it exceeds 0 °C. However, in this study, the daily temperature effect was calculated according to Yin et al. [49], and the DFL of each accession was converted to the sum of the daily temperature effect (SDTE) by the summation of each daily temperature effect "*g(T)*" from sowing to flowering.

$$g(T) = \left(\frac{T_c - T}{T_c - T_o}\right)\left(\frac{T - T_b}{T_o - T_b}\right)^{\frac{T_o - T_b}{T_c - T_o}}$$

where *g(T)* is the daily temperature effect, T is the daily mean temperature, T_b (0 °C) is the barley base temperature, T_o (21 °C) is the barley optimal temperature, and T_c (35 °C) is the barely ceiling temperature according to Cao and Moss [44], Tamaki et al. [45], and, Ellis et al. [46].

2.3. Statistical Analyses

The statistical analysis of flowering data was performed with the statistics package SAS 9.4 software [50]. The analysis of DFL, DRFL, and SDTE, as well as average, minimum and maximum temperature was conducted using the *proc means* procedure. Additionally, the procedure *proc mixed* was used for the ANOVA and estimation of least-square means (*lsmeans*) for DFL, DRFL, and SDTE. The model was fit with selected parameters as the dependent variable; accessions and locations were fixed effects, while year, replication, and blocks were random effects. The effect of accessions' interaction with location was also included as a fixed effect to estimate the *lsmeans* of each variable.

As parameters were evaluated at one location over different years, repeatability (r^2) was used to evaluate the adaptability and stability of the accessions. The '*lme4*' R package [51,52] was applied to compute the variance components and repeatability (r^2) of traits recorded for more than one year. The variance in accession ($\sigma^2{}_G$), residual variance components ($\sigma^2 e$), number of replications (*rep*), and number of years (*ny*) were used to calculate repeatability as follows:

$$r^2 = \sigma^2_G / (\sigma^2_G + \frac{\sigma^2}{ny \times rep})$$

The frequency and regression analysis was conducted using Microsoft excel 2016 software. The frequency of days above the optimal temperature (21 °C) as well as the frequency of chilling days that fulfill the respective chilling temperature requirement were analyzed for each year and location and compared with the average flowering time as well as with the flowering response. Moreover, the regression analysis between the frequency of days above the optimal temperature with the average DFL of a specific location as well as the frequency of chilling days with the percentage of non-flowered plots was also conducted.

The Pearson correlation coefficient analysis between DFL and DRFL, as well as DFL and SDTE, was conducted with the statistics package SAS 9.4 software [50] using the *proc corr* procedure.

2.4. Genome Wide Association Studies (GWAS)

A set of 10,644 highly polymorphic SNP markers [41] as well as the *lsmeans* of phenotype data of DRFL and SDTE with the correction factor of population structure ("PCA.total = 3") were used to conduct GWAS using the "Bayesian information and Linkage-disequilibrium Iteratively Nested Keyway (BLINK)" model [53] in R v.4.1.2 software [54]. Benjamini and Hochberg [55] considered markers significant if they surpass a false discovery rate (FDR) adjusted *p*-value of <0.05, and this standard was used in this study.

Significant markers obtained from the GWAS analysis were further analyzed using the LD decay value of each chromosome, as reported in Teklemariam et al. [41], and if the

SNP markers were within the LD decay value, the marker with the smallest p-value was selected to represent the respective QTL. The logarithm of the odds (LOD) was calculated for the significant markers with a "–log (*p*-value)". The significant QTLs were mapped using MapChart 2.32 software [56], and the functional annotation of significant markers was analyzed by BARLEYMAP version 3 [57] against the Morex genome v2 [36].

3. Results

3.1. Analysis of Weather Conditions

The highest maximum mean temperature during the flowering time evaluation period was observed at MK (28.2 °C), while the lowest minimum mean temperature was observed at HL (7.9 °C). In CC, the lowest mean maximum temperature (20.4 °C) and the highest mean minimum temperature (15.2 °C) compared with all field experiment locations was observed. The presence of a very high coefficient of variation for the minimum temperature across all field locations indicated the presence of a wider range of minimum temperatures (Table S1).

In all experimental locations, the maximum temperature was below T_c and above T_b. (Table S1). The HL and CC experiments were carried out at an optimal temperature (0 to 28 °C) throughout the experimental period, followed by DZ, at which 95% of experimental days were in the optimal temperature range. MK had the least optimal growth temperature, with only 46% of the days falling in the range of optimal growth conditions (Figure 1).

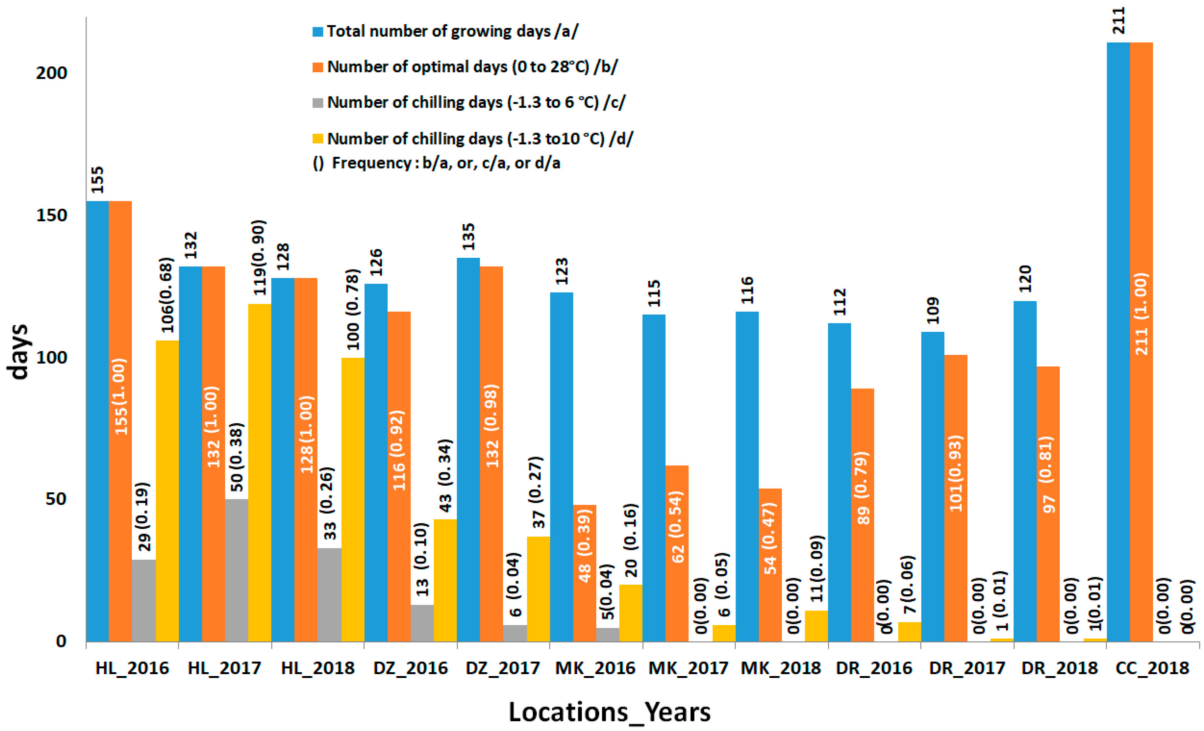

Figure 1. The number of growing days, days with optimal temperatures (0 to 28 °C), and days with chilling temperature (−1.3 to 6 °C; and −1.3 to 10 °C), along with their corresponding frequency values. Experimental locations are DZ = Debrezeit, DR = Dera, HL = Holetta, MK = Melkassa, and CC = climate chamber.

According to defined chilling requirement criteria [47], HL had the highest percentage (27%) of chilling days, while CC and DR had the lowest (0.0%). When the effective vernalization temperature increased from 6 to 10 °C, 78% of growing days at HL could be defined as chilling days, while the lowest number of days was observed at CC and DR, with 0 and 3% of days, respectively (Figure 1).

3.2. Evaluation of Flowering Status

The phenotypic diversity in the 260 Ethiopian barley landrace accessions during the time of flowering was observed in each trial. In the field experiments, the highest mean of DFL was recorded at HL (72.4 d), which was 8, 11, and 15 d longer than in DZ, DR, and MK, respectively. The mean DFL of the CC experiment was 109.5 d, which was on average 42% or 46 d longer than the average DFL (63.8 d) of all field locations, at which the least difference was observed in HL (37 d), while the highest variation was in MK (52 d). Moreover, the CC experiment was also the one with the highest standard deviation as well as coefficient of variance compared with all field locations, followed by DZ and MK (Table 2).

Table 2. Descriptive statistics for days to flowering, days to reverse flowering, and summation of daily temperature effect.

	Location	Mean	Std Dev	Min.	Max.	Variance	Std Error	CV	LSD	Repeatability
DFL	DZ	64.1	10.5	41.0	97.0	111.0	0.27	16.4	6.7	92.5
	DR	61.2	9.2	39.0	101.0	84.6	0.19	15.0	5.5	93.3
	HL	72.4	8.0	50.0	98.0	64.8	0.17	11.1	3.4	96.4
	MK	57.6	9.6	38.0	105.0	93.0	0.20	16.7	5.4	93.4
	CC	109.5	22.5	70.0	210.0	506.6	0.82	20.6	21.2	-
DRFL	DZ	71.7	11.4	0.0	95.0	130.4	0.29	15.9	7.6	85.5
	DR	60.6	14.7	0.0	85.0	215.4	0.30	24.2	8.9	93.3
	HL	82.5	8.2	0.0	105.0	67.7	0.17	10.0	3.6	96.0
	MK	64.5	12.4	0.0	86.0	154.9	0.26	19.3	7.9	90.1
	CC	119.6	28.9	0.0	162.0	834.8	1.03	24.2	27.6	-
SDTE	DZ	62.8	10.3	40.3	95.0	106.5	0.26	16.4	6.5	92.5
	DR	60.5	9.0	38.7	99.8	81.4	0.19	14.9	5.4	93.3
	HL	63.0	7.2	43.8	85.7	51.7	0.15	11.4	3.0	96.4
	MK	57.2	9.6	37.8	105.3	91.6	0.20	16.7	5.3	93.3
	CC	100.8	22.0	63.2	199.7	484.3	0.80	21.8	20.8	-

Legend: Experimental locations are DZ = Debrezeit, DR = Dera, HL = Holetta, MK = Melkassa, and CC = climate chamber; Std Dev = standard deviation, Min. = minimum value, Max. = maximum value, Std Error = standard error, CV = coefficient of variation, LSD = the least significant difference; traits analyzed are DFL = days to flowering, DRFL = days to reverse flowering, and SDTE = sum of daily temperature effect. Reduction calculated for reduction percentage with the following formula: (mean of DFL − mean of SDTE)/mean of DFL) × 100.

When the DFL data were converted to DRFL, the highest CV was recorded for DR and CC. This is due to few accessions in DR and CC that did not flower in contrast to other locations (Figure 2). Although the result of SDTE seems in harmony with DFL, the mean SDTE difference between each field location was the smallest compared with DFL except for HL, where the SDTE value was reduced by 13% compared to DFL, while the lowest reduction was observed at MK, DR, and DZ in the range of 0.6 to 2.0% (Table 2).

Flowering (Z58) at MK began at the 6th week after sowing (WAS), while it started on the 7th WAS at DR and DZ. The latest flowering response under field conditions was observed at HL (8th WAS). Most of the accessions at MK, DZ, and DR flowered on the 9th WAS, while it was on the 10th WAS at HL. The flowering pattern in the CC, in contrast, differed from field experiments, in which Z49 was started on the 11th WAS and the peak flower response was noted on the 15th WAS (Figure 2).

The highest proportion of non-flowering plots (3.5%) was observed for DR and the highest flowering response was recorded for HL (Figure 2; Table S2). The presence of such a low flowering response at DR could also be associated with the presence of drought stress at this location [41]. Although the longer dry spell at DR and MK started in the month of September [58–60], accessions at MK flowered on average 4 days earlier than at DR (Table 2), which could be associated with the presence of a higher day temperature than at DR (Table S1).

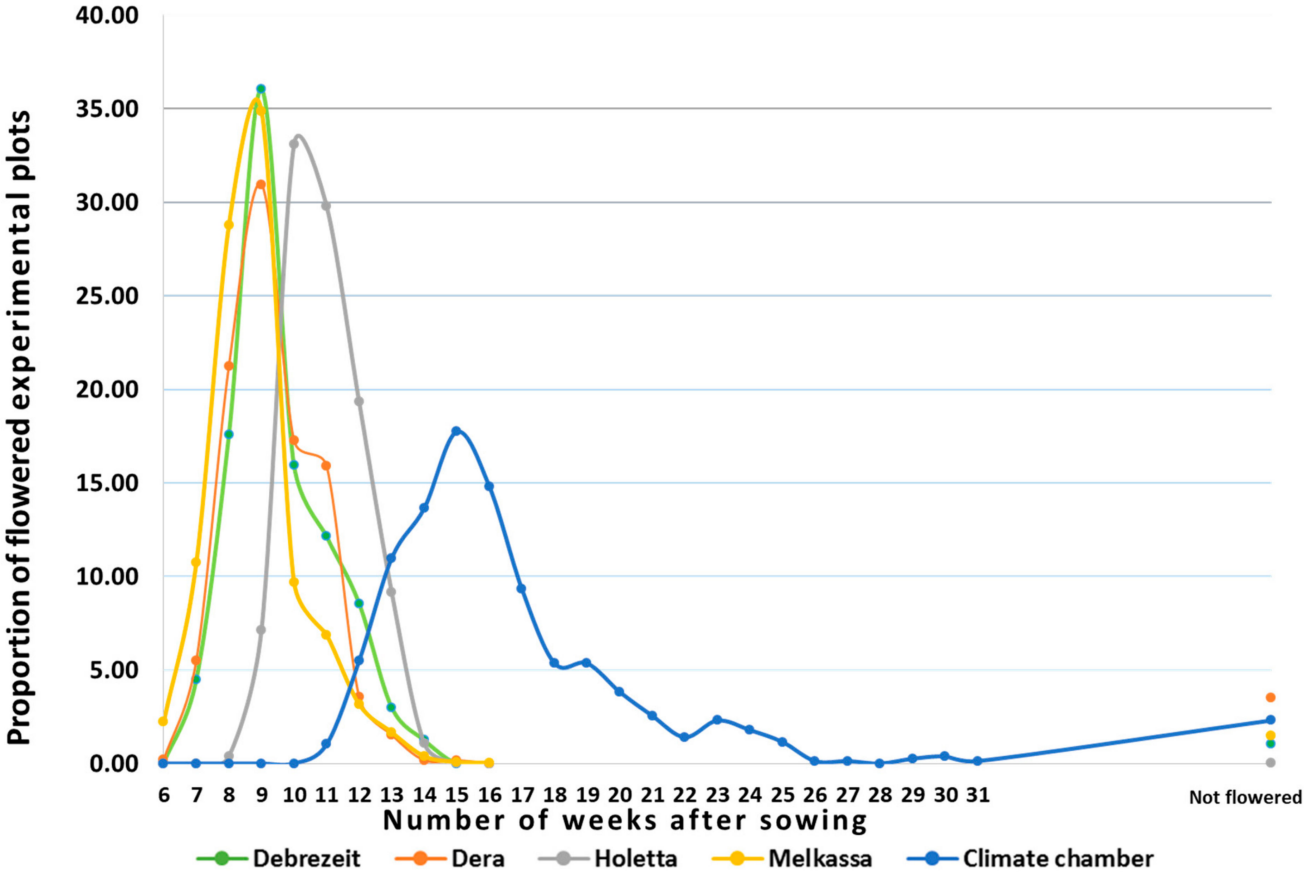

Figure 2. Percentage (proportion) of flowering plots in each experimental field location (Z58) and for climate chamber experimental pots (Z49) throughout the experimental period (weeks).

3.3. Repeatability

The repeatability of DFL, DRFL, and SDTE parameters was high in all field experimental locations. The least observed repeatability of DFL was for DZ (92.5%) and the highest was for HL (96.4%). The highest repeatability for DRFL was for HL (96.0%), and the least was for DZ (85.5%), while for SDTE the highest was for HL (96.4%) and the lowest was for DZ (92.5%). The repeatability of CC was not analyzed, as the experiment was conducted for one year only (Table 2). The presence of a high repeatability as well as variation among accessions provided an excellent intervention point to study the genetics of the flowering time in Ethiopian accessions in detail.

3.4. Correlation and Regression Analysis

The DFL of Ethiopian barley landraces was observed to be very strongly and positively associated with most agronomic traits investigated during the drought stress experiment conducted at the field and climate chamber experiments [41].

The Pearson correlation coefficient (r) of DFL and DRFL among the field experiment locations was positive and highly significant ($p < 0.001$). The highest correlation for DFL was between DR and MK ($r = 0.92$, $p < 0.001$), while the lowest was between DR and HL ($r = 0.82$, $p < 0.001$). For DRFL, the highest was between DR and MK ($r = 0.93$, $p < 0.001$) and the lowest was between DR and HL ($r = 0.80$, $p < 0.001$) (Table 3). Although a positive and significant correlation ($p < 0.001$) was observed for both DFL and DRFL in CC and field trials, the r value was much lower than the r values observed between field sites. The smallest r value of DFL between CC and field trials was found for HL ($r = 0.49$, $p < 0.001$) and the highest for MK ($r = 0.57$, $p < 0.001$), while for DRFL, the highest ($r = 0.55$, $p < 0.001$) and the lowest ($r = 0.44$, $p < 0.001$) correlations were found for MK and HL,

respectively (Table 3). This might be associated with the presence of the highest values for standard deviation, variance, and CV for both variables in CC compared to all field sites (Tables 2, 3 and S1).

Table 3. Pearson correlation coefficient (*r*) between the field and climatic chamber experiments using Ethiopian barley accessions. Days to flowering are shown above the diagonal cells, while correlations for days to reverse flowering are listed below the diagonal cells; *** significant at $p < 0.001$.

		DFL				
		CC	**DZ**	**DR**	**HL**	**MK**
DRFL	CC		0.53 ***	0.55 ***	0.49 ***	0.57 ***
	DZ	0.50 ***		0.88 ***	0.89 ***	0.91 ***
	DR	0.52 ***	0.86 ***		0.82 ***	0.92 ***
	HL	0.44 ***	0.89 ***	0.75 ***		0.85 ***
	MK	0.55 ***	0.89 ***	0.93 ***	0.80 ***	

Legend: Experimental locations are DZ = Debrezeit, DR = Dera, HL = Holetta, MK = Melkassa, and CC = climate chamber; traits analyzed are DFL = days to flowering, and DRFL = days to reverse flowering.

The maximum temperature was recorded above T_b (0 °C) in all experimental locations, while a chilling temperature below T_{bc} (−1.3 °C) was observed only for 4 d at HL during 2016. The minimum temperature was also above T_{bc} in all locations (Table S3). Therefore, a frequency below 1 for optimal growth conditions was due to the presence of above T_o (28 °C), which ultimately shortened the average flowering days in DZ, DR, and MK compared to HL (Figures 1 and 3a). Similarly, a frequency below 1 for chilling days was primarily due to the presence of temperatures above T_{oc} (6 °C or 10 °C), which appears to be associated with the flowering of all accessions or with the lowest non-flowering proportion of accessions in each location (Figures 1 and 3b,c).

The regression analysis indicated that the daily maximum temperature explained about 32% of flowering time in Ethiopian accessions (Figure 3a). Additionally, the presence of an optimal chilling temperature below 6 °C contributed about 56% to complete flowering of all accessions, while in the case that the optimal chilling temperature was assumed to be below 10 °C, its contribution increased to 65% (Figure 3b,c).

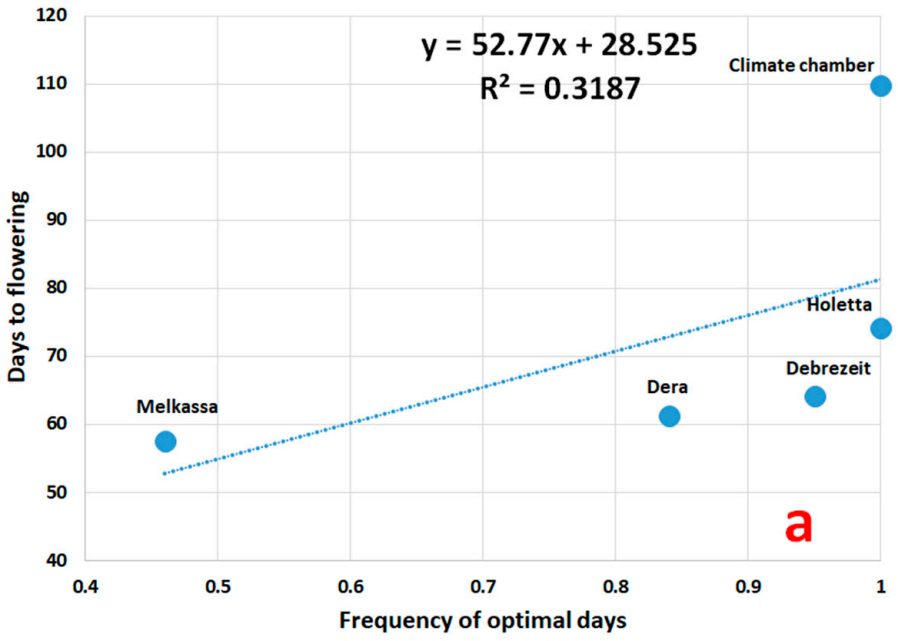

Figure 3. *Cont.*

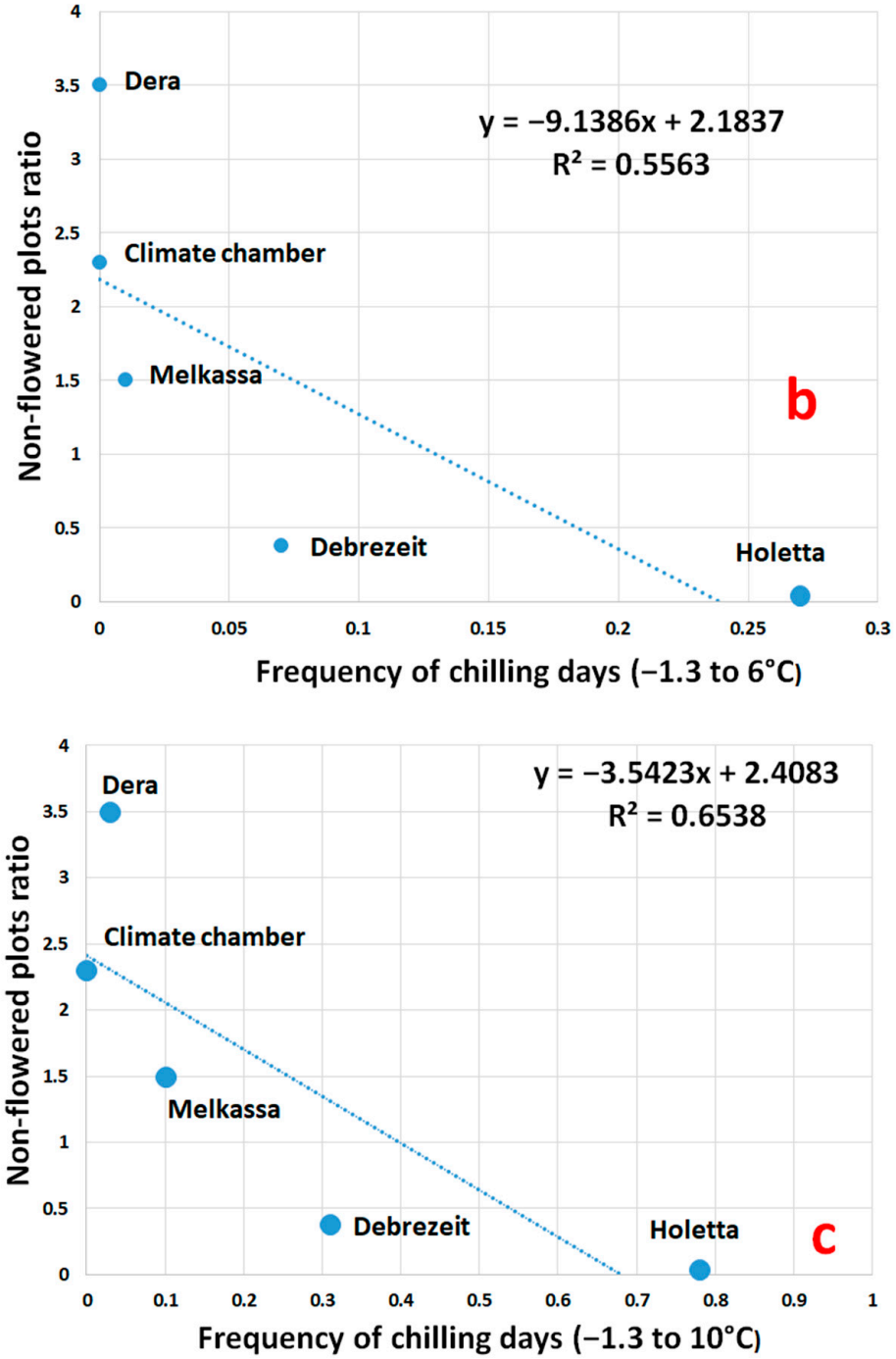

Figure 3. Regression analysis between daily temperature and flowering proportion: (**a**) based on optimal temperature (T_o); (**b**) based on optimal chilling temperature requirement (T_{bc} = 6 °C); and (**c**) based on optimal chilling temperature requirement (T_{bc} = 10 °C).

3.5. Analysis of Variance (ANOVA)

The ANOVA results for DFL, DRFL, and SDTE of the four field locations revealed significant variation ($p < 0.001$) between locations, accessions, as well as the interaction of accessions and locations. The presence of significant variation between accessions of CC was also observed (Table 4).

Table 4. F values from ANOVA of flowering time of field and climate chamber experiments and morphological parameters of field experiments.

Experiment	Effects		DRFL	DFL	SDTE
Field	Accessions (A)	F value	34.24 ***	40.96 ***	40.00 ***
		DF	259	259	259
	Location (L)	F value	3429.55 ***	2759.16 ***	388.63 ***
		DF	3	3	3
	A X L	F value	2.25 ***	1.72 ***	1.85 ***
		DF	777	777	777
Climate chamber	Accessions	F value	4.76***	4.63 ***	4.64 ***
		DF	195	195	195

Legend: Experimental locations are from field (Debrezeit, Dera, Holetta, and Melkassa), and climate chamber; traits analyzed are DRFL for days to reverse flowering, DFL for days to flowering, and SDTE for sum of daily temperature effect. DF stands for degree of freedom; and "***" indicate significance at p-value < 0.001 probability level.

Based on the *lsmeans* of accessions at each location, the 20 earliest and the 20 latest flowering accessions were sorted. The common number of accessions obtained in the drought-prone locations (MK and DR) was 13/20 for the latest and 14/20 for the earliest flowering accessions. Similarly, 15/20 of the earliest and 11/20 of the latest flowering accessions were common for the optimal moisture locations (DZ and HL). Overall, only nine out of twenty of the earliest and four out of twenty of the latest common flowering accessions were found in all field trial locations. The CC had only two out of twenty common late-flowering accessions with drought-prone locations and no common earliest accessions with all field experiment locations (Table S4). The mean DFL values of every accession in the CC were found to be higher than the mean DFL values of every other accession in the MK, DZ, DR, and HL sites, with the exception of 3, 8, 10, and 10 of the earliest accessions in the CC (Table S4).

3.6. Genome Wide Association Study Analysis of Flowering Time Traits

The presence of three distinct structural populations and the LD decay values of each chromosome have already been described in Teklemariam et al. [41], and, Teklemariam et al. [42].

The correlation analysis between one location of SDTE and DFL indicated that the two parameters were similar, as the r values were 1 (Table S5). A GWAS analysis was therefore conducted for SDTE and DRFL. Combined multiple-year data of each location and one-year data from the CC were used during the analysis. Most of the GWAS results were found to be well-fitted to the BLINK model, as seen by the Quantile–quantile (QQ) plots (Figure S1). Based on FDR values, 40 marker trait associations (MTAs) were identified, of which 23 MTAs were for DRFL, while 17 MTAs were for SDTE (Tables 5 and S6). When the detected MTAs were further assigned to putative QTLs based on the LD decay value of each chromosome [41], a total of 39 QTLs were detected, of which 22 QTLs were for DRFL and 17 QTLs for SDTE. Since all QTLs, except one for DRFL of CC on chromosome 4H 3.6–4.1 Mb, were represented by one MTA (Tables 5 and S6), the findings of this study will center on MTAs.

Table 5. List of MTAs for flowering time of Ethiopian barley landraces under four field experimental locations in Ethiopia and climate chamber using BLINK models.

No	SNP	Chr	Pos (Mbp)	MAF	LOD	Effect	PVE (%)	Loc	Trait	QTL	Gene Ontologies	Annotation Description
1	JHI-Hv50k-2016-12926	1H	13.73	0.32	5.2	−1.14	0.45	MK	SDTE	MKSDTE1	GO:0005488	Armadillo/beta-catenin-like repeat protein
2	SCRI_RS_116548	1H	24.03	0.08	6.5	−1.59	1.49	HL	SDTE	HLSDTE1		Unknown protein; located in endomembrane system; BEST *Arabidopsis thaliana* protein match is an unknown protein
3	JHI-Hv50k-2016-18950	1H	59.28	0.08	6.7	−4.26	2.70	DR	DRFL	DRDRFL1	GO:0016887 GO:0042626 GO:0055085 GO:0005524 GO:0006810 GO:0016021	Lipid A export ATP-binding/permease protein MsbA
4	JHI-Hv50k-2016-18950	1H	59.28	0.08	10.2	3.17	4.27	MK	SDTE	MKSDTE2	GO:0016887 GO:0042626 GO:0055085 GO:0005524 GO:0006810 GO:0016021	Lipid A export ATP-binding/permease protein MsbA
5	JHI-Hv50k-2016-26918	1H	369.36	0.10	5.9	6.32	4.83	CC	SDTE	CCSDTE1	GO:0005515	Leucine-rich repeat family protein
6	JHI-Hv50k-2016-26982	1H	371.70	0.31	7.3	7.72	1.91	CC	DRFL	CCDRFL1		Abscisic acid receptor *PYR1*
7	JHI-Hv50k-2016-31649	1H	427.69	0.09	6.8	10.46	4.16	CC	DRFL	CCDRFL2		RNA recognition motif-containing protein
8	JHI-Hv50k-2016-72079	2H	25.15	0.27	6.2	−1.28	2.81	HL	SDTE	HLSDTE2	GO:0016020 GO:0055085 GO:0005215 GO:0006810 GO:0006811	Cation-chloride cotransporter 2
9	JHI-Hv50k-2016-73570	2H	29.31	0.19	7.6	−9.32	2.12	CC	DRFL	CCDRFL3		Undescribed protein
10	JHI-Hv50k-2016-73570	2H	29.31	0.19	11.2	8.27	5.27	CC	SDTE	CCSDTE2		Undescribed protein
11	JHI-Hv50k-2016-111156	2H	678.19	0.03	5.1	−8.63	9.22	CC	SDTE	CCSDTE3	GO:0006486 GO:0016757	Hexosyltransferase

Table 5. *Cont.*

No	SNP	Chr	Pos (Mbp)	MAF	LOD	Effect	PVE (%)	Loc	Trait	QTL	Gene Ontologies	Annotation Description
12	JHI-Hv50k-2016-147628	2H	766.08	0.07	6.0	−2.57	2.34	MK	SDTE	MKSDTE3	GO:0008270	*RING/FYVE/PHD* zinc finger superfamily protein
13	JHI-Hv50k-2016-148133	2H	767.33	0.07	8.2	5.06	5.79	DR	DRFL	DRDRFL2		
14	JHI-Hv50k-2016-151505	3H	4.06	0.14	4.6	3.18	0.81	DR	DRFL	DRDRFL3		
15	JHI-Hv50k-2016-151820	3H	4.57	0.11	5.6	−9.19	1.97	CC	DRFL	CCDRFL4	GO:0043531	Disease resistance protein
16	JHI-Hv50k-2016-198140	3H	596.97	0.16	5.0	4.64	2.16	CC	SDTE	CCSDTE4	GO:0004553 GO:0005975 GO:0030246	Beta-galactosidase 10
17	JHI-Hv50k-2016-206858	3H	643.17	0.04	6.0	−14.85	2.66	CC	DRFL	CCDRFL5	GO:0005515 GO:0008270	RING/U-box superfamily protein
18	JHI-Hv50k-2016-213204	3H	662.66	0.03	5.6	16.46	3.55	CC	DRFL	CCDRFL6		UV-stimulated scaffold protein A homolog
19	JHI-Hv50k-2016-213207	3H	662.66	0.03	6.3	−13.06	4.77	CC	SDTE	CCSDTE5		
20	SCRI_RS_188420	3H	681.79	0.29	7.1	1.21	1.75	HL	DRFL	HLDRFL1	GO:0051861 GO:0005737 GO:0017089 GO:0046836	Kinesin-like protein/Silicon efflux transporter
21	JHI-Hv50k-2016-227500	4H	3.24	0.09	5.9	−6.18	3.53	CC	SDTE	CCSDTE6		Chromosome 3B, genomic scaffold, cultivar Chinese Spring
22	JHI-Hv50k-2016-227517	4H	3.57	0.09	4.7	8.32	2.98	CC	DRFL	CCDRFL7		Unknown function
23	JHI-Hv50k-2016-227778	4H	4.06	0.11	4.7	7.67	2.44	CC	DRFL	CCDRFL7		Very-long-chain (3R)-3-hydroxyacyl-CoA dehydratase
24	SCRI_RS_188340	4H	471.65	0.39	6.7	6.48	1.22	CC	DRFL	CCDRFL8		Vacuolar protein-sorting-associated protein 37 homolog 2
25	JHI-Hv50k-2016-259986	4H	595.53	0.04	5.6	−4.54	4.75	MK	DRFL	MKDRFL1		
26	JHI-Hv50k-2016-281308	5H	10.63	0.04	5.4	3.04	1.73	DZ	SDTE	DZSDTE1	GO:0005515	F-box protein/undescribed protein
27	JHI-Hv50k-2016-310148	5H	510.24	0.25	5.6	2.33	1.10	DR	DRFL	DRDRFL4		Ribosomal L5P family protein
28	JHI-Hv50k-2016-323294	5H	571.62	0.32	5.7	−1.69	1.26	DZ	DRFL	DZDRFL1	GO:0003700 GO:0006355 GO:0043565	ABSCISIC ACID-INSENSITIVE 5-like protein 2

Table 5. *Cont.*

No	SNP	Chr	Pos (Mbp)	MAF	LOD	Effect	PVE (%)	Loc	Trait	QTL	Gene Ontologies	Annotation Description
29	JHI-Hv50k-2016-323294	5H	571.62	0.32	5.6	−1.46	0.85	MK	DRFL	MKDRFL2	GO:0003700 GO:0006355 GO:0043565	ABSCISIC ACID-INSENSITIVE 5-like protein 2
30	JHI-Hv50k-2016-323294	5H	571.62	0.32	5.9	1.20	0.76	MK	SDTE	MKSDTE4	GO:0003700 GO:0006355 GO:0043565	ABSCISIC ACID-INSENSITIVE 5-like protein 2
31	JHI-Hv50k-2016-323294	5H	571.62	0.32	8.6	1.78	1.38	DR	SDTE	DRSDTE1	GO:0003700 GO:0006355 GO:0043565	ABSCISIC ACID-INSENSITIVE 5-like protein 2
32	JHI-Hv50k-2016-323571	5H	572.54	0.36	4.9	1.98	0.44	DR	DRFL	DRDRFL5	GO:0042176 GO:0000502 GO:0005515 GO:0030234/GO:0006468 GO:0004672 GO:0005515 GO:0005524	26S proteasome non-ATPase regulatory subunit 3 homolog A/Leucine-rich receptor-like protein kinase family protein
33	JHI-Hv50k-2016-345406	5H	623.06	0.30	6.6	1.64	0.51	DZ	DRFL	DZDRFL2	GO:0005515	U3 small nucleolar RNA-associated protein 18 homolog
34	JHI-Hv50k-2016-367393	5H	668.61	0.25	4.6	−3.91	1.01	CC	SDTE	CCSDTE7	GO:0043531	Disease resistance protein
35	JHI-Hv50k-2016-378408	6H	19.55	0.35	5.0	−2.19	0.42	DR	DRFL	DRDRFL6		Unknown function
36	JHI-Hv50k-2016-397916	6H	348.23	0.03	5.2	5.73	3.67	DR	DRFL	DRDRFL7		GDP-L-galactose phosphorylase 2
37	JHI-Hv50k-2016-410857	6H	499.35	0.50	6.5	5.71	1.22	CC	DRFL	CCDRFL9		Unknown function/undescribed protein
38	JHI-Hv50k-2016-422808	6H	558.86	0.03	14.5	9.14	15.39	MK	DRFL	MKDRFL3	GO:0003676 GO:0005634	CCR4-NOT transcription complex subunit 7
39	JHI-Hv50k-2016-449688	7H	14.61	0.24	4.9	1.30	0.66	MK	SDTE	MKSDTE5	GO:0008152 GO:0016758	UDP-Glycosyltransferase superfamily protein
40	JHI-Hv50k-2016-457708	7H	32.79	0.34	7.2	1.64	0.95	DR	SDTE	DRSDTE2	GO:0003676 GO:0003677	Unknown function

Legend: SNP = names of SNP marker associated; Chr = chromosome; Loc = locations (HL = Holetta, DZ = Debrezeit, DR = Dera, MK = Melkassa, and CC = climate chamber); Trait = traits (DRFL= days to reverse flowering; and SDTE = sum of daily temperature effect); MAF = minor allele frequency; PVE (%) = percentage of phenotype variance explained; LOD is logarithm of odds calculated as LOD = −log (*p*-value); Gene Ontologies and Annotation description are based on Morex genome v2 [29].

For each barley chromosome, at least two associations with a flowering time of Ethiopian barley's accession were detected, despite the presence of variations in the number of MTA distributions between chromosomes. The chromosome 5H had the highest number of MTAs (9), while chromosome 7H had the least (2) (Table S7).

MTAs with the highest three LOD values are on chromosome 6H at 658.9 Mb (14.5) for DRFL at MK, chromosome 2H at 29.3 Mb (11.2) for SDTE at CC, and chromosome 1H at 59.3 Mb (10.2) for SDTE at MK (Table S6). The three highest marker effect values were recorded at CC, for MTAs on chromosome 3H at 643.2 Mb for DRFL (−14.85), at 662.66 Mb for SDTE (−13.06) and DRFL (16.46), and on chromosome 1H at 427.7 Mb for DRFL (10.46). The presence of the highest standard deviations, variance, and LSD values in the CC (Table 2), could potentially contribute to the highest marker effect values in the CC (Tables 5 and S6). MTAs with the highest percentage of phenotype variance explained (PVE) values are on chromosome 6H at 558.9 Mb for DRFL of MK (15.39) and on chromosome 2H at 678.2 Mb for SDTE of CC (9.22) (Tables 5 and S6).

There were three common markers that were detected for at least more than one parameter or location (Table S6). The "JHI-Hv50k-2016-323294" marker, which was located on chromosome 5H at 571.62 Mb, was detected for the SDTE of MK and DR and DRFL of DZ, DR, and MK. The remaining two were the "JHI-Hv50k-2016-18950" marker on chromosome 1H at 59.3 Mb detected for the SDTE of MK and DRFL of DR, and the "JHI-Hv50k-2016-73570" marker on chromosome 2H at 29.3 Mb detected for SDTE and DRFL of CC (Tables 5 and S6).

Although there were no common markers detected between the field and CC, a QTL was detected on chromosome 3H at 4.1–4.6 Mb for the DRFL of DR and CC (Figure 4 and Table S6). Four QTLs were overlapped between the SDTE and DRFL of CC on chromosome 1H-4H, while two QTLs were detected between DR and MK on chromosome 1H and 2H; the rest were between CC and DR on chromosome 3H, and between DZ, MK, and DR on chromosome 5H (Figure 4 and Table S6).

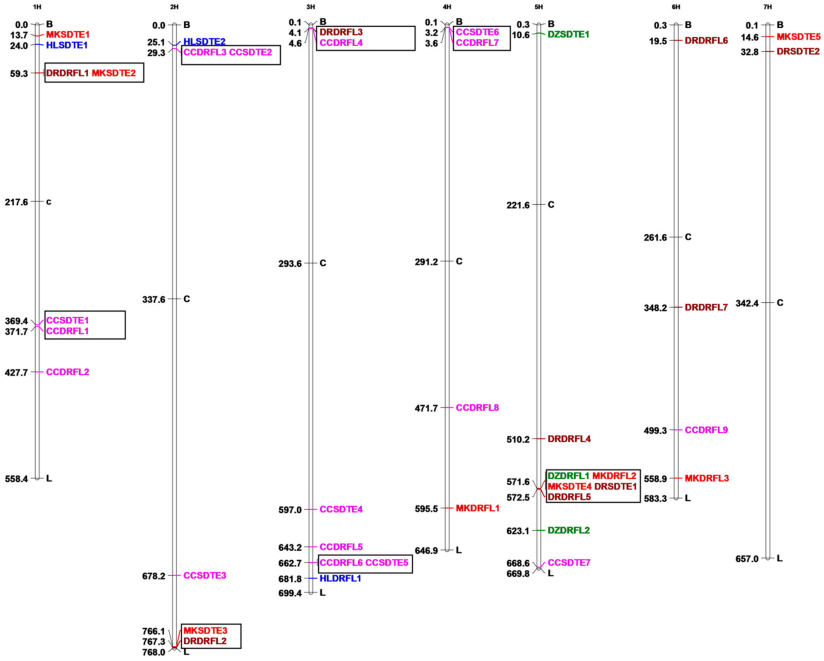

Figure 4. Genetic map showing significant QTLs of Ethiopian barley landrace accessions associated with days to reverse flowering (DRFL) and summation of daily temperature effect (SDTE). The physical distance in Mbp; C = centromere region of the chromosome; B and L = known start and stop position of chromosomes based on [36]; QTL in blue font for Holetta, green font for Debrezeit, red font for Melkassa, brown for Dera, and purple font for climate chamber experimental location detected using the BLINK model.

4. Discussion

4.1. Phenotypic Variation on Flowering Time

The flowering time is an important and complex trait that is controlled by a number of genetic networks and environmental signals [10,16]. The flowering time of Ethiopian barley accessions was evaluated in this study at different locations of Ethiopia that had varying daily temperatures and annual precipitation. The study was also conducted in the climate chamber that had a constant day and night temperature. In previous research, Tsehaye et al. [35] also studied the flowering time on Ethiopian barley landraces in both long and short days and reported the role of major flowering genes.

The flowering pattern of a worldwide barley collection was studied in Japan at the same field location for 20 seasons [61]. According to the results, the genotype accounted for the majority of the variation in flowering time, with the geographic origin being second. The interaction between genotype with environment and geographic origin with environment explained about 90% and 55% of the variation in flowering time, respectively.

Although Ethiopian barleys in the Sato et al. [61] study formed a genetically distinct cluster, they did not show a different flowering pattern compared with other geographic origins. However, about 25% of Ethiopian materials in the study were included in the group of Japanese local materials based on their stable flowering pattern performance in varying environments across different seasons. The insensitivity of Ethiopian materials to the photoperiod was explained as the reason for their stable flowering pattern in that study.

Altitude and atmospheric temperature typically have an inverse relationship. Although there was a significant difference in minimum temperature across the different altitudes of barley growing areas in Ethiopia, the coldest months of the year (October to January) do not fall in either of the two cropping seasons: the main season '*meher*', which is from June to September, and the minor season '*belg*', which is from February to April. Therefore, in both cropping seasons, the landraces were assumed to be not exposed to the vernalization temperature requirement for flower initiation. As a result, Ethiopian barleys are considered as spring types that did not require strong vernalization temperatures and a critical photoperiod length to flower [32].

Our experiments conducted at four locations in Ethiopia with different environmental conditions (Table 1) and in the climate chamber also confirmed that accessions are independent from the requirement of a strong vernalization temperature, but there is a significant difference in the flowering time (Table 4 and Figure S2). Notably, the flowering time of the accessions appear to be more dependent on the thermal time (growing degree-days (GDD) [°C d]) (Figure 3a), which refers to the summation of the total temperature required to reach the flowering stage [28,29].

Global warming is a major concern for sustainable agricultural production in the world, and Solomon [62] forecasted that global temperatures will increase by 1.8 to 4.0 °C at the end of this century. The lowest altitude (1550 masl) and warmest location in our study is MK, while the highest altitude (2400 masl) and coldest location is HL (Table 1). The average temperature variation between DR and MK, DZ and DR, and HL and DZ is about 1.1 °C, 1.7 °C, and 3.7 °C, respectively (Table 1). Therefore, the field experiment in these four locations enables us to predict how global warming would affect barley production in Ethiopian conditions.

Nevo et al. [63] studied the global warming effect on flowering patterns of 10 wild barley ancestral populations from the 1980s with their descendant populations from 2008. The result indicated that the descendant population flowered earlier than the ancestral population. A subsequent study by Qian et al. [64] suggested that the fixation of SNP/Indels in major flowering regions of the descendant populations contributed to early flowering in the changing environment.

The flowering time of the latest accessions groups was more affected by the variation in temperature in the four experimental locations, as only four of twenty common accessions between them were found, in contrast to nine of twenty common accessions in the earliest accessions groups (Table S4). Moreover, accessions at MK flowered earliest, while they

flowered latest at HL. Previous studies conducted in Ethiopia also demonstrated that the mean flowering time at Sheno (2800 masl) was 84.6 d [35], while it was 87.3 d at Ankober (2970 masl) [65], and barley landraces were reported to mature between 7 and 9 months in the extreme highlands of Ethiopia (>3500 masl) (personal communication).

Hemming et al. [66] revealed barley genotypes flowering earlier at 25 °C than at 15 °C. Karsai et al. [67] grew barley genotypes at a constant day temperature of 9 to 18 °C and at a 2 °C lower night temperature and demonstrated that a 1 °C increase in temperature resulted in a 5.2 d earlier flowering time. White et al. [68], and, Dixon et al. [69] also reported a significant shortening of the flowering time in wheat when the ambient temperature increased.

In addition, the presence of fluctuating temperatures of 18/16 °C day/night delayed flowering time by up to 71 d in spring-type barley genotypes compared with a constant temperature of 18 °C [67]. In a 20-season research project conducted at the same location in Japan, the Ethiopian barley genotypes' flowering time ranged from 145 to 165 [61]. The DFL of accessions in the CC was delayed for an average maximum and minimum of 52 and 37 d in comparison to MK and HL, respectively (Table 2), which is lower than the 71 d reported by Karsai et al. [67], while the observed range of DFL (70–210 d) was wider than the findings from the field study of Sato et al. [61].

In addition to the primary factors like the photoperiod and vernalization, additional critical factors may be required for the timely flowering of barley [70]. Hence, for the Ethiopian accessions, critical alternative factors might be the presence of a wide range of day/night temperature variation and/or ambient daily maximum temperatures of >21 °C. In contrast to the CC, where temperature fluctuation between day and night was 4 °C and showed a significantly delayed flowering time, our field experiments showed a temperature fluctuation of >10 °C on the majority of days (Table S3).

The negative influence of higher atmospheric temperature on the grain yield of barley was discussed in different studies using long photoperiods [71,72]. Morphological parameters like plant height, spike length, and flag leaf length were reported to be influenced by elevated temperatures over the optimal range [73]. According to Zhu et al. [74], during early barley development, elevated temperature promotes plant length; in the later developmental stage, plants grown at an elevated temperature become shorter compared to plants grown at an optimal temperature. However, the elevated temperature has at the same time insignificant effects on leaf length and leaf width. The effect of atmospheric temperature on some morphological parameters of Ethiopian barley accessions was also assessed in our study using correlation analysis. The findings revealed that the experimental location's atmospheric temperature difference has a significant effect on both the plant height and flag leaf length, as accessions at warm locations (MK and DR) had been shorter in plant height and flag leaf length compared with the cold location HL. However, it has less of an effect on spike length (Table S8).

Earliness is one of the drought tolerance mechanisms, in which genotypes escape the adverse drought stress and complete the lifecycle before the onset of a longer dry period [75]. Vaezi et al. [76], Barati et al. [77], and, Forster et al. [78] demonstrated the negative association of the flowering time with grain yield during a drought stress period. Our previous study also confirmed a strong negative correlation of DFL with grain biomass in drought stress treatments [41]. Compared with other experimental locations, MK and DR exhibited the highest frequency of days above the optimal average daily temperature (21 °C), with values of 0.69 and 0.37, respectively (Table S3), which favor accelerated vegetative growth, and benefited early flowering accession to complete their lifecycle before the occurrence of a drought spell.

The developmental transition of barley from the vegetative stage to the reproductive stage is significantly influenced by drought stress [79,80]. The presence of adverse drought conditions at MK and DR seriously affected flowering. This can be witnessed by the presence of a very low ratio of non-flowering plots during 2017, when a very good distribution of rainfall was observed at each location compared with other seasons (Tables S2 and S4).

In the climate chamber experiment, most accessions had difficulties to complete the transition to flowering from Z49, i.e., awn tipping to Z58, i.e., spike emergence (Figure S3). While such an effect was also observed in both water treatments, it was more pronounced in the drought stress treatment (86% of the plot failed to transit to Z58) than in the optimal moisture treatment (30% of the plot failed the transition) (Table S9). A quartile analysis was used to further analyze the failure of the Z49–Z58 transition. The highest percentage of early flowering accessions (88% and 24%) from the first quartile of control and drought stress treatments, respectively, completed the flowering stage transition. In the subsequent quartiles, the percentage of completed flowering stage transitions decreased gradually, and the lowest percentage was found for the latest flowering accessions in the fourth quartile (21% and 4%), respectively, for drought stress and control treatments (Table S9). The effect of drought stress on the developmental transition of barley genotypes from the vegetative stage to the reproductive stage was also discussed in Su et al. [79], and, Gol et al. [80].

The highest correlation coefficient between flowering time and days to maturity (DM) of the drought stress treatments and control treatments in both the field and climate chamber experiments was reported in Teklemariam et al. [41]. The correlation between drought stress and control treatments for corresponding accessions was analyzed. The DM of the climatic chamber drought stress treatment has a significant correlation with the DM of DR and MK at $p < 0.001$ ($r = 0.42$ and $r = 0.49$), respectively. In contrast, the DM of the CC control treatment exhibited the lowest correlation coefficient with the DM of HL ($r = 0.15$) compared to the DM of all field locations, although it had a significant correlation at $p < 0.05$ (Table S9). The low correlation coefficient between the cool and naturally optimal moisture location (HL) and CC control treatment, compared to warm and naturally optimal moisture (DZ) and drought-prone (DR and MK) locations, indicates that in addition to an optimal soil moisture content, the atmospheric conditions of the cool agro-ecologies of Ethiopia play a role in determining the morphological growth parameters.

Yin et al. [49] reported an average of 66.09 SDTE for two varieties; and the range of 57 to 80 SDTE was reported for 94 barley recombinant breeding lines [81]. In our study, the mean SDTE was 57.2 to 63.0 in field trial locations, while the mean of the CC was 100.8 (Table 2).

4.2. Flowering Time Associated Marker Under Different Environments

Chromosome 2H, 5H, and 7H were identified as important chromosomes, which are strongly associated with the flowering time of barley [40,82–84]. Yin et al. [81] also identified chromosome 1H, 2H, and 3H as important chromosomes associated with barley SDTE. In our study, most MTAs for flowering time were detected on chromosome 5H, but also on chromosome 1H, 2H, and 3H. (Tables S6 and S7; and Figure 4).

In our study, the detected MTAs corresponded to 35 genes, of which, for 19, at least one Gene Ontology (GO) term (Table S6) was found. A GO term enrichment analysis was conducted using "The Singular Enrichment Analysis tool in GO analysis toolkit and database for the agricultural community, AgriGO v2.0" (https://systemsbiology.cpolar.cn/agriGOv2/index.php, accessed on 26 July 2024) [85]. Based on both the Bonferroni adjusted *p*-value and the non-adjusted method, no significantly enriched GO term was identified. The absence of enriched significant GO terms in our study could be associated with the identified GO terms, may not be properly annotated with the corresponding terms [86].

The dominant flowering gene of barley '*Ppd-H1*' promotes flowering under longer days, while plants with the recessive *ppd-H1* allele remain vegetative during long days [10,17,27]. The MTAs for the SDTE and DRFL were found in the CC on chromosome 2H at 29.3 Mb (Tables 5 and S6). Upstream of '*Ppd-H1*' at 21.6 Mb, the '*GBM1035*' marker, which is identified with a genebank ID of '*AL500260*' on https://wheat.pw.usda.gov/GG3/ (accessed on 22 May 2023), promotes flowering in wild barley *H. spontaneum* [87]. The MTA for the SDTE of HL, which has cool weather conditions with adequate rainfall and a longer growing season (4 months), was identified between the '*Ppd-H1*' gene and the '*GBM1035*' marker at 25.1 Mb (Table 5 and Figure 4). Caproni et al. [37] reported an MTA around this

flowering gene in the barley growing highlands of Ethiopia, with an elevation of 2000–2400 masl.

Cosenza et al. [16] reported the presence of a cluster of QTLs around *Ppd-H1* from 22.3 to 31.3 Mb, which are associated with flowering time and plant height; they suggested that these QTLs might have a small effect on the control of this trait. Therefore, the reported MTAs at 25.1 Mb in HL and 29.3 Mb in the CC might have a related effect on determining the flowering time.

Some of the telomere regions of chromosomes have significant MTAs with the flowering time of Ethiopian barley, as significant MTAs were found close to the telomere regions of chromosomes 2H, 3H, 4H, and 5H (Figure 4). Alqudah et al. [27] also reported significant MTAs associated with different flowering time-related traits on similar telomeres regions of chromosomes for photoperiod-sensitive genotypes; however, it was not reported for non-sensitive genotypes. Significant MTAs at the telomere of 3H were also reported in Kikuchi et al. [88].

The only locus that overlapped between the field and CC experimental locations was found on chromosome 3H, for DR and CC, at 4.1 to 4.6 Mb (Table 5). Alqudah et al. [27] reported the association of a marker for awn tipping (Z49) at 4.2 Mb of chromosome 3H. Kikuchi et al. [88] also reported a marker known as '*HvMFT1*', which was mapped at 2.4 Mb of chromosome 3H, which has a poor association with flowering time. A distinct difference in the temperature conditions between the CC and field locations (Table S2) may account for the few overlapping loci, and this is also explained by the lower correlation coefficient (*r*) value between the CC and field locations compared to the *r* value between field locations (Table 3). Teklemariam et al. [41] also reported a few overlapping MTAs between the field and CC for different traits in drought stress experiments.

An MTA was found for DRFL on chromosome 1H at 427.7 Mb, which has an association with the flowering time in the CC experiment (Table 5 and Figure 4). He et al. [89] identified the *HvPAF* (*HORVU1Hr1G058630*) gene close to this locus at 427.9 Mb, which is associated with a phytochrome-A-associated F-box protein and has a role in light perception and signaling in the flowering pathway. This MTA was also identified in Teklemariam et al. [41] for grain biomass, harvest index, and thousand kernel weight in a climate chamber experiment at an optimal moisture treatment.

The drought stress during the vegetative developmental stage of barley revealed that genotypes that carry the recessive *ppd-H1* allele were observed to significantly delay flowering time in comparison to wild-type *Ppd-H1* allele [90]. On the other hand, during high ambient temperatures, recessive *ppd-H1* barley was observed to accelerate the flowering time with the background *Vrn-H1* allele [71,72].

The major genes that differentiate winter barley from spring barley are mapped on chromosome 5H as '*Vrn-H1*' at 599.1 Mb [10,22] and a rice ortholog flowering gene, '*HD6-5H*', mapped at 531.6 Mb [91]. The circadian clock gene,'*HvPRR95*', was mapped at 565.15 Mb, and reported to be expressed during the evening of a long day, while its expression is reduced due to osmotic stress [92]; and Ford et al. [93] also reported an increasing trend of *HvPRR95* gene expression with the increase in temperature.

In our study, MTAs, which determine the flowering time at the warm location of DZ, DR, and MK, were consistently detected on chromosome 5H at 571.6 to 572.5 Mb with a gene ID of '*HORVU5Hr1G084260*' and a protein description of "abscisic acid-insensitive 5-like (*Abl5*) protein 2" for MTA at 571.6 Mb (Table S6). Thiel et al. [94] also describe the role of this gene in flower organ formation. The *Arabidopsis* ortholog gene '*AT4G35900*' promotes flower initiation in the wild-type allele, while it delays the flowering time in the mutant [95]. Additionally, Finkelstein [96] explained that *AbI5* delayed flower initiation by prohibiting lateral root formation through ABA-dependent nitrate inhibition. The association of this locus with grain biomass at an optimal moisture condition as well as days to maturity of drought condition was reported for the field experiment in Teklemariam et al. [41].

Moreover, due to the difference in day length between the Australian and European environments, *HvPRR95* was reported to have a significant role compared to *Ppd-H1* by

Pham et al. [9], and also reported to have an effect on elevated temperature [93]. Therefore, the consistent detection of MTAs close to the *HvPRR95* circadian clock gene could be associated with the presence of the significant day length between the Ethiopian environment and high latitude regions and/or the higher temperature at the warmer locations of DZ, DR, and MK.

A significant MTA on chromosome 5H for the CC was detected at 668.6 Mb for the STDE (Table 5 and Figure 4). Upstream of this MTA, *FRIGIDA*, which is known to have pleiotropic effects for environmental adaptation during drought stress [38], was mapped at 662.6 Mb by Mascher et al. [36]. Caproni et al. [37] also reported the effect of this MTA on the flowering time of Ethiopian barley landraces.

Specifically, the flowering time of Ethiopian barley landraces were studied at the molecular level by Tsehaye et al. [35], and, Caproni et al. [37]. In our study, the GWAS analysis was used to identify MTAs that have a direct influence on the flowering time of Ethiopian barley; however, to utilize these MTAs as breeding targets of barley's flowering time, validations of MTAs in a controlled environment will be required to develop high-resolution markers.

5. Conclusions

The vernalization temperature had no effect on the flowering time of Ethiopian barley landraces, as expected. This study identified GDDs as the major influencing factor in determining the flowering response in Ethiopian barley accessions. The presence of warm atmospheric temperatures accelerated the accession's vegetative growth, resulting in the shortest number of days to flowering in MK, DR, and DZ. The early flower response of the accessions in all field experiment locations compared to the CC may be associated with the presence of an optimal day temperature of >21 °C and a fluctuating temperature >10 °C between day/night. Furthermore, because all accessions consistently flowered at HL, few landraces might require mild chilling temperatures of at least 11 to 13 °C to complete flowering. The locus on chromosome 5H at 571.6 to 572.5 Mb has a strong association with the flowering time in warm areas, while the two loci on chromosome 2H at 25.1 Mb and 29.3 Mb could have an influence on the flowering time at the colder HL location and the CC, respectively. While this study provided broad insights into factors (GDD, >21 °C daily temperature, and extended rainfall) affecting the flowering time of Ethiopian barley accessions and identified significant MTAs, more research in controlled environments with distinct variations in all possible factors and detailed research on the interaction between the identified MTAs and known major flowering genes will pinpoint the exact factors related to Ethiopian barley landrace accession flowering times.

Supplementary Materials: The following are available online at https://www.mdpi.com/article/10.3390/agronomy14123031/s1, Table S1: Summarized experimental location weather data. Legend: "MaxTemp" = mean maximum temperature, "MinTemp" = mean minimum temperature, "AvTemp" = mean of daily average temperature; Std Dev = standard deviation, Minimum = minimum value, Maximum = maximum value, Std Error = standard error, CV = coefficient of variation; CC = climate chamber, DZ = Debrezeit, DR = Dera, HL = Holetta, MK = Melkassa; Table S2: Ethiopian barley landrace flowering response at the field of the four locations from 2016–2018 and climate chamber 2018 experiment. Legend: DZ = Debrezeit, DR = Dera, HL = Holetta, MK = Melkassa, CC = climate chamber; Table S3: Summary weather data of experimental locations during the experimental period; Table S4: The top and bottom 20 accessions in each location for flowering (DFL = days to flowering, Acc = Accessions, CC = climate chamber, DR = Dera, DZ = Debrezeit, HL = Holetta, MK = Melkassa). The shared top 20 are highlighted by red boxes, the shared bottom 20 are highlighted by blue boxes, and those shared between CC, MK, and DR are highlighted by purple boxes; Table S5: Person correlation coefficient (r) for days to flowering and sum of daily temperature effect based on 260 Ethiopian barley landraces in field experiments. Above the diagonal line correlation result for sum of daily temperature effect (SDTE); below diagonal line correlation result for days to flowering (DFL); and on the diagonal line correlation between SDTE and DFL of the same locations; *** significant at $p < 0.001$. Legend: DZ = Debrezeit, DR = Dera, HL = Holetta, MK = Melkassa, CC = climate chamber;

Table S6: List of significant MTAs obtained using BLINK model analysis for GWAS analysis to detect associations with flowering time of 260 and 196 Ethiopia barley landrace accessions in field and climate chamber experiments, respectively, using 10,644 SNP markers; listed are MTA (SNP), related genomic region (QTL), candidate gene identifiers, and annotations. Remark: SNP markers detected for more than one location or parameter are highlighted with blue color, SNP markers with distance less than the LD decay value of the chromosome are circled with bold rectangular line; QTL markers represented by more than one SNP marker are highlighted with green color; Table S7: Number of detected MTAs that determine the flowering time of Ethiopian barley across the barley genome and identified influential/consistently detected loci (chromosome 1H to 7H); Table S8: Person correlation coefficient (r) of flowering time (DFL for days to flowering), and DRFL for days to reverse flowering) of Ethiopian barley landraces with some morphological parameters (FLL for flag leaf length, PH for plant height, SL for spike length) for the individual field locations; *** significant at $p < 0.001$, ** significant at $p < 0.01$, * significant at $p < 0.05$, and ns for non-significant; Table S9: Quartile analysis for awn tipping (Z49) and complete emergence of spike (Z58); and Person correlation analysis (r) of days to maturity for 196 Ethiopian barley landraces between the field and climatic chamber experiments using Ethiopian barley accessions. Legend: DM = days to maturity, DZ = Debrezeit, DR = Dera, HL = Holetta, MK = Melkassa, CC = climate chamber, Dr = drought stress treatments, Con = control treatments; Figure S1: Quantile–quantile (QQ) plots of GWAS for barley drought tolerance using BLINK model analysis; Legend: "CC" for climate chamber; "DZ" for Debrezeit; "DR" for Dera; "HL" for Holetta; "MK" for Melkassa, "SDTE" for summation daily temperature effect; "DRFL" for days to reverse flowering; Figure S2: Morphological growth of Ethiopian barley (Z11—early germination or Z12 from two leaf emerged; Z31—first node formation and Z49—main spike awn visible) at field experiments (a = Holetta location, and b = Melkassa location) and c = climate chamber experiment; Figure S3: Flowering of Ethiopian barley in the climate chamber (a = control plot (left) completed Z58 stage; drought stressed plot (right) failed to reach Z58 stage; b = both control (left) and stressed (right) plots failed to reach Z58 stage).

Author Contributions: The concept for the study was designed by F.O. and G.W. The study's conception and design involved input from all authors. S.S.T., K.N.B. and G.W. prepared the study materials, collected the data, and carried out the analysis. The supervision was provided by F.O., K.P., A.M. and G.W., S.S.T. conducted the data analysis and wrote the initial draft of the paper; the other authors provided feedback on earlier drafts. All authors have read and agreed to the published version of the manuscript.

Funding: The funding of this research project (FKZ 2813FS01) was provided by the Federal Ministry of Food and Agriculture (BMEL, Bundesministerium für Ernährung und Landwirtschaft).

Data Availability Statement: The original contributions presented in this study are included in the article/Supplementary Materials. Further inquiries can be directed to the corresponding author(s).

Acknowledgments: The authors would like to express gratitude the Ethiopian Biodiversity Institute (EBI) and the Holetta Agricultural Research Center (HARC) for providing the initial planting materials. Our appreciation also goes out to the laboratory and greenhouse technicians and administrative staff of the Julius Kühn Institute (JKI), and EIAR personnel of the individual research stations. Eshetu Zewdu (EIAR) provided summarized meteorological data of each field station, Zeray Mehari (MIDROC Investment Group) assisted with GO term enrichments, and Heike Lehnert (JKI) and Habte Nida (Perdue University) helped with data analysis; all of these individuals deserve special appreciation. We finally thank the Bundesministerium für Ernährung und Landwirtschaft (BMEL), the Federal Ministry of Food and Agriculture, for financing this study.

Conflicts of Interest: Author Andrea Matros was employed by the company COMPOLYTICS GmbH. The remaining authors declare that the research was conducted in the absence of any commercial or financial relationships that could be construed as a potential conflict of interest.

References

1. CSA. *Agricultural Sample Survey 2018/2019*; Central Statistical Agency: Addis Ababa, Ethiopia, 2019.
2. Yaynu, H. (Ed.) Response of barley landraces to low-moisture stress in a lowrainfall environment. In *Barley Research and Development in Ethiopia, Proceedings of the 2nd National Barley Research and Development Review Workshop, Holetta, Ethiopia, 28–30 November 2006*; Holetta Agricultural Research Centre, Ethiopian Institute of Agricultural Research: Holeta, Ethiopia; International Center for Agricultural Research in the Dry Areas (ICARDA): Beirut, Lebanon, 2006.

3. Mohammed, J.; Seleshi, S.; Nega, F.; Lee, M. Revisit to Ethiopian traditional barley-based food. *J. Ethn. Foods* **2016**, *3*, 135–141. [CrossRef]
4. Royo, C.; Ammar, K.; Alfaro, C.; Dreisigacker, S.; del Moral, L.F.G.; Villegas, D. Effect of *Ppd-1* photoperiod sensitivity genes on dry matter production and allocation in durum wheat. *Field Crops Res.* **2018**, *221*, 358–367. [CrossRef]
5. Göransson, M.; Hallsson, J.H.; Lillemo, M.; Orabi, J.; Backes, G.; Jahoor, A.; Hermannsson, J.; Christerson, T.; Tuvesson, S.; Gertsson, B.; et al. Identification of Ideal Allele Combinations for the Adaptation of Spring Barley to Northern Latitudes. *Front. Plant Sci.* **2019**, *10*, 542. [CrossRef]
6. Alqudah, A.M.; Schnurbusch, T. Heading Date Is Not Flowering Time in Spring Barley. *Front. Plant Sci.* **2017**, *8*, 896. [CrossRef] [PubMed]
7. Cuesta-Marcos, A.; Casas, A.M.; Hayes, P.M.; Gracia, M.P.; Lasa, J.M.; Ciudad, F.; Codesal, P.; Molina-Cano, J.L.; Igartua, E. Yield QTL affected by heading date in Mediterranean grown barley. *Plant Breed.* **2009**, *128*, 46–53. [CrossRef]
8. Esparza Martínez, J.H.; Foster, A.E. Genetic analysis of heading date and other agronomic characters in barley (*Hordeum vulgare* L.). *Euphytica* **1998**, *99*, 145–153. [CrossRef]
9. Pham, A.-T.; Maurer, A.; Pillen, K.; Taylor, J.; Coventry, S.; Eglinton, J.K.; March, T.J. Identification of wild barley derived alleles associated with plant development in an Australian environment. *Euphytica* **2020**, *216*, 148. [CrossRef]
10. Cockram, J.; Chiapparino, E.; Taylor, S.A.; Stamati, K.; Donini, P.; Laurie, D.A.; O'Sullivan, D.M. Haplotype analysis of vernalization loci in European barley germplasm reveals novel VRN-H1 alleles and a predominant winter VRN-H1/VRN-H2 multi-locus haplotype. *Theor. Appl. Genet.* **2007**, *115*, 993–1001. [CrossRef] [PubMed]
11. Kikuchi, R.; Handa, H. Photoperiodic control of flowering in barley. *Breed. Sci.* **2009**, *59*, 546–552. [CrossRef]
12. Laurie, D.A.; Pratchett, N.; Snape, J.W.; Bezant, J.H. RFLP mapping of five major genes and eight quantitative trait loci controlling flowering time in a winter × spring barley (*Hordeum vulgare* L.) cross. *Genome* **1995**, *38*, 575–585. [CrossRef]
13. Snape, J.W.; Sarma, R.; Quarrie, S.A.; Fish, L.; Galiba, G.; Sutka, J. Mapping genes for flowering time and frost tolerance in cereals using precise genetic stocks. *Euphytica* **2001**, *120*, 309. [CrossRef]
14. Maurer, A.; Draba, V.; Jiang, Y.; Schnaithmann, F.; Sharma, R.; Schumann, E.; Kilian, B.; Reif, J.C.; Pillen, K. Modelling the genetic architecture of flowering time control in barley through nested association mapping. *BMC Genom.* **2015**, *16*, 290. [CrossRef] [PubMed]
15. Fernández-Calleja, M.; Casas, A.M.; Igartua, E. Major flowering time genes of barley: Allelic diversity, effects, and comparison with wheat. *Theor. Appl. Genet.* **2021**, *134*, 1867–1897. [CrossRef] [PubMed]
16. Cosenza, F.; Shrestha, A.; Van Inghelandt, D.; Casale, F.A.; Wu, P.-Y.; Weisweiler, M.; Li, J.; Wespel, F.; Stich, B. Genetic mapping reveals new loci and alleles for flowering time and plant height using the double round-robin population of barley. *J. Exp. Bot.* **2024**, *75*, 2385–2402. [CrossRef]
17. Hemming, M.N.; Peacock, W.J.; Dennis, E.S.; Trevaskis, B. Low-temperature and daylength cues are integrated to regulate FLOWERING LOCUS T in barley. *Plant Physiol.* **2008**, *147*, 355–366. [CrossRef] [PubMed]
18. Turner, A.; Beales, J.; Faure, S.; Dunford, R.P.; Laurie, D.A. The Pseudo-Response Regulator *Ppd-H1* Provides Adaptation to Photoperiod in Barley. *Science* **2005**, *310*, 1031–1034. [CrossRef] [PubMed]
19. Casao, M.C.; Karsai, I.; Igartua, E.; Gracia, M.P.; Veisz, O.; Casas, A.M. Adaptation of barley to mild winters: A role for PPDH2. *BMC Plant Biol.* **2011**, *11*, 164. [CrossRef] [PubMed]
20. Trevaskis, B.; Hemming, M.N.; Dennis, E.S.; Peacock, W.J. The molecular basis of vernalization-induced flowering in cereals. *Trends Plant Sci.* **2007**, *12*, 352–357. [CrossRef]
21. Trevaskis, B.; Bagnall, D.J.; Ellis, M.H.; Peacock, W.J.; Dennis, E.S. MADS box genes control vernalization-induced flowering in cereals. *Proc. Natl. Acad. Sci. USA* **2003**, *100*, 13099–13104. [CrossRef]
22. Fu, D.; Szűcs, P.; Yan, L.; Helguera, M.; Skinner, J.S.; von Zitzewitz, J.; Hayes, P.M.; Dubcovsky, J. Large deletions within the first intron in VRN-1 are associated with spring growth habit in barley and wheat. *Mol. Genet. Genom.* **2005**, *273*, 54–65. [CrossRef]
23. Cockram, J.; Hones, H.; O'Sullivan, D.M. Genetic variation at flowering time loci in wild and cultivated barley. *Plant Genet. Resour.* **2011**, *9*, 264–267. [CrossRef]
24. von Bothmer, R.; Sato, K.; Komatsuda, T.; Yasuda, S.; Fischbeck, G. Chapter 2—The domestication of cultivated barley. In *Developments in Plant Genetics and Breeding*; Von Bothmer, R., van Hintum, T., Knüpffer, H., Sato, K., Eds.; Elsevier: Amsterdam, The Netherlands, 2003; Volume 7, pp. 9–27. [CrossRef]
25. Borràs-Gelonch, G.; Slafer, G.A.; Casas, A.M.; van Eeuwijk, F.; Romagosa, I. Genetic control of pre-heading phases and other traits related to development in a double-haploid barley (*Hordeum vulgare* L.) population. *Field Crops Res.* **2010**, *119*, 36–47. [CrossRef]
26. Slafer, G.A.; Molina-Cano, J.L.; Savin, R.; Araus, J.L.; Romagosa, I. *Barley Science: Recent Advances from Molecular Biology to Agronomy of Yield and Quality*; Food Products Press: Binghamton, NY, USA, 2003.
27. Alqudah, A.M.; Sharma, R.; Pasam, R.K.; Graner, A.; Kilian, B.; Schnurbusch, T. Genetic dissection of photoperiod response based on GWAS of pre-anthesis phase duration in spring barley. *PLoS ONE* **2014**, *9*, e113120. [CrossRef]
28. McMaster, G.S.; Wilhelm, W.W. Growing degree-days: One equation, two interpretations. *Agric. For. Meteorol.* **1997**, *87*, 291–300. [CrossRef]
29. Miller, P.; Lanier, W.; Brandt, S. Using Growing Degree Days to Predict Plant Stages. In *Ag/Extension Communications Coordinator, Communications Services*; Montana State University-Bozeman: Bozeman, MO, USA, 2001; Volume 59717, pp. 994–2721.

30. Juskiw, P.E.; Jame, Y.-W.; Kryzanowski, L. Phenological Development of Spring Barley in a Short-Season Growing Area. *Agron. J.* **2001**, *93*, 370–379. [CrossRef]
31. Ibrahim, A.; Harrison, M.; Meinke, H.; Fan, Y.; Johnson, P.; Zhou, M. A regulator of early flowering in barley (*Hordeum vulgare* L.). *PLoS ONE* **2018**, *13*, e0200722. [CrossRef] [PubMed]
32. Saisho, D.; Ishii, M.; Hori, K.; Sato, K. Natural Variation of Barley Vernalization Requirements: Implication of Quantitative Variation of Winter Growth Habit as an Adaptive Trait in East Asia. *Plant Cell Physiol.* **2011**, *52*, 775–784. [CrossRef]
33. Knüpffer, H.; Terentyeva, I.; Hammer, K.; Kovaleva, O.; Sato, K. Ecogeographical diversity—A Vavilovian appraoch. *Dev. Plant Genet. Breed.* **2003**, *7*, 53–76. [CrossRef]
34. Yang, J.; Wang, J.; Jia, Q.; Zhu, J. Barley breeding and production in China. In *Cereals China*; CIMMYT: Mexico City, Mexico, 2010; Volume 69.
35. Tsehaye, Y.; Bjørnstad, Å.; Abay, F. Phenotypic and genotypic variation in flowering time in Ethiopian barleys. *Euphytica* **2012**, *188*, 309–323. [CrossRef]
36. Mascher, M.; Gundlach, H.; Himmelbach, A.; Beier, S.; Twardziok, S.O.; Wicker, T.; Radchuk, V.; Dockter, C.; Hedley, P.E.; Russell, J.; et al. A chromosome conformation capture ordered sequence of the barley genome. *Nature* **2017**, *544*, 427. [CrossRef] [PubMed]
37. Caproni, L.; Lakew, B.F.; Kassaw, S.A.; Miculan, M.; Ahmed, J.S.; Grazioli, S.; Kidane, Y.G.; Fadda, C.; Pè, M.E.; Dell'Acqua, M. The genomic and bioclimatic characterization of Ethiopian barley (*Hordeum vulgare* L.) unveils challenges and opportunities to adapt to a changing climate. *Glob. Change Biol.* **2023**, *29*, 2335–2350. [CrossRef]
38. Lovell, J.T.; Juenger, T.E.; Michaels, S.D.; Lasky, J.R.; Platt, A.; Richards, J.H.; Yu, X.; Easlon, H.M.; Sen, S.; McKay, J.K. Pleiotropy of FRIGIDA enhances the potential for multivariate adaptation. *Proc. R. Soc. B Biol. Sci.* **2013**, *280*, 20131043. [CrossRef] [PubMed]
39. Hemming, M.N.; Fieg, S.; James Peacock, W.; Dennis, E.S.; Trevaskis, B. Regions associated with repression of the barley (*Hordeum vulgare*) VERNALIZATION1 gene are not required for cold induction. *Mol. Genet. Genom.* **2009**, *282*, 107–117. [CrossRef] [PubMed]
40. Wang, G.; Schmalenbach, I.; von Korff, M.; Léon, J.; Kilian, B.; Rode, J.; Pillen, K. Association of barley photoperiod and vernalization genes with QTLs for flowering time and agronomic traits in a BC2DH population and a set of wild barley introgression lines. *Theor. Appl. Genet.* **2010**, *120*, 1559–1574. [CrossRef] [PubMed]
41. Teklemariam, S.S.; Bayissa, K.N.; Matros, A.; Pillen, K.; Ordon, F.; Wehner, G. Genome wide association study of Ethiopian barley for terminal drought stress tolerance under field and climate chamber conditions. *Cereal Res. Commun.* **2023**, *52*, 1731–1750. [CrossRef]
42. Teklemariam, S.S.; Bayissa, K.N.; Matros, A.; Pillen, K.; Ordon, F.; Wehner, G. The genetic diversity of Ethiopian barley genotypes in relation to their geographical origin. *PLoS ONE* **2022**, *17*, e0260422. [CrossRef] [PubMed]
43. Zadoks, J.C.; Chang, T.T.; Konzak, C.F. A decimal code for the growth stages of cereals. *Weed Res.* **1974**, *14*, 415–421. [CrossRef]
44. Cao, W.; Moss, D.N. Temperature Effect on Leaf Emergence and Phyllochron in Wheat and Barley. *Crop Sci.* **1989**, *29*, 1018–1021. [CrossRef]
45. Tamaki, M.; Kondo, S.; Itani, T.; Goto, Y. Temperature responses of leaf emergence and leaf growth in barley. *J. Agric. Sci.* **2002**, *138*, 17–20. [CrossRef]
46. Ellis, R.H.; Roberts, E.H.; Summerfield, R.J.; Cooper, J.P. Environmental Control of Flowering in Barley (*Hordeum vulgare* L.). II. Rate of Developement as a Function of Temperature and Photoperiod and its Modification by Low-temperature Vernalization. *Ann. Bot.* **1988**, *62*, 145–158. [CrossRef]
47. Chujo, H. Studies of vernalization in wheat and barley plants, especially on effects of factors on the vernalization of growing plants. *Bull. Univ. Osaka Prefect. B* **1975**, *27*, 253–310.
48. Porter, J.R.; Gawith, M. Temperatures and the growth and development of wheat: A review. *Eur. J. Agron.* **1999**, *10*, 23–36. [CrossRef]
49. Yin, X.; Struik, P.C.; Tang, J.; Qi, C.; Liu, T. Model analysis of flowering phenology in recombinant inbred lines of barley. *J. Exp. Bot.* **2005**, *56*, 959–965. [CrossRef] [PubMed]
50. SAS Institute. *Base SAS® 9.4 Procedures Guide*, 7th ed.; SAS Institute: Cary, NC, USA, 2019.
51. Bates, D.; Mächler, M.; Bolker, B.; Walker, S. Fitting linear mixed-effects models using lme4. *arXiv* **2014**, arXiv:1406.5823.
52. R Core Team. *R Version 3.6.1. A Language and Environment for Statistical Computing*; R Foundation for Statistical Computing: Vienna, Austria, 2019. Available online: http://www.R-project.org/ (accessed on 23 February 2020).
53. Huang, M.; Liu, X.; Zhou, Y.; Summers, R.M.; Zhang, Z. BLINK: A package for the next level of genome-wide association studies with both individuals and markers in the millions. *Giga Sci.* **2018**, *8*, giy154. [CrossRef] [PubMed]
54. R Core Team. *R Version 4.2.1. A Language and Environment for Statistical Computing*; R Foundation for Statistical Computing: Vienna, Austria, 2021. Available online: http://www.R-project.org/ (accessed on 21 November 2022).
55. Benjamini, Y.; Hochberg, Y. Controlling the False Discovery Rate—A Practical and Powerful Approach to Multiple Testing. *J. R. Stat. Soc. B Met.* **1995**, *57*, 289–300. [CrossRef]
56. Voorrips, R.E. MapChart: Software for the graphical presentation of linkage maps and QTLs. *J. Hered.* **2002**, *93*, 77–78. [CrossRef]
57. Cantalapiedra, C.P.; Boudiar, R.; Casas, A.M.; Igartua, E.; Contreras-Moreira, B. BARLEYMAP: Physical and genetic mapping of nucleotide sequences and annotation of surrounding loci in barley. *Mol. Breed.* **2015**, *35*, 13. [CrossRef]
58. Kassie, B.T.; RÖTter, R.P.; Hengsdijk, H.; Asseng, S.; Van Ittersum, M.K.; Kahiluoto, H.; Van Keulen, H. Climate variability and change in the Central Rift Valley of Ethiopia: Challenges for rainfed crop production. *J. Agric. Sci.* **2013**, *152*, 58–74. [CrossRef]

59. Bekele, D.; Alamirew, T.; Kebede, A.; Zeleke, G.; M Melesse, A. Modeling Climate Change Impact on the Hydrology of Keleta Watershed in the Awash River Basin, Ethiopia. *Environ. Model. Assess.* **2019**, *24*, 95–107. [CrossRef]
60. Bekele, D.; Alamirew, T.; Kebede, A.; Zeleke, G.; Melese, A.M. Analysis of rainfall trend and variability for agricultural water management in Awash River Basin, Ethiopia. *J. Water Clim. Change* **2016**, *8*, 127–141. [CrossRef]
61. Sato, K.; Ishii, M.; Takahagi, K.; Inoue, K.; Shimizu, M.; Uehara-Yamaguchi, Y.; Nishii, R.; Mochida, K. Genetic Factors Associated with Heading Responses Revealed by Field Evaluation of 274 Barley Accessions for 20 Seasons. *iScience* **2020**, *23*, 101146. [CrossRef] [PubMed]
62. Solomon, S. *Climate Change 2007—The Physical Science Basis: Working Group I Contribution to the Fourth Assessment Report of the IPCC*; Cambridge University Press: Cambridge, UK, 2007.
63. Nevo, E.; Fu, Y.-B.; Pavlicek, T.; Khalifa, S.; Tavasi, M.; Beiles, A. Evolution of wild cereals during 28 years of global warming in Israel. *Proc. Natl. Acad. Sci. USA* **2012**, *109*, 3412–3415. [CrossRef] [PubMed]
64. Qian, C.; Yan, X.; Shi, Y.; Yin, H.; Chang, Y.; Chen, J.; Ingvarsson, P.K.; Nevo, E.; Ma, X.-F. Adaptive signals of flowering time pathways in wild barley from Israel over 28 generations. *Heredity* **2020**, *124*, 62–76. [CrossRef] [PubMed]
65. Yigzaw, D. *Genotype by Environment Interaction and Stability of Malt Barley (*Hordeum vulgare *L.) Varieties Across Major Growing Areas of Amhara Region, Ethiopia*; Bahirdar University: Bahirdar, Ethiopia, 2021.
66. Hemming, M.N.; Walford, S.A.; Fieg, S.; Dennis, E.S.; Trevaskis, B. Identification of high-temperature-responsive genes in cereals. *Plant Physiol.* **2012**, *158*, 1439–1450. [CrossRef]
67. Karsai, I.; Kőszegi, B.; Kovács, G.; Szűcs, P.; Mészáros, K.; Bedő, Z.; Veisz, O. Effects of temperature and light intensity on flowering of barley (*Hordeum vulgare* L.). *Acta Biol. Hung.* **2008**, *59*, 205–215. [CrossRef]
68. White, J.W.; Kimball, B.A.; Wall, G.W.; Ottman, M.J.; Hunt, L.A. Responses of time of anthesis and maturity to sowing dates and infrared warming in spring wheat. *Field Crops Res.* **2011**, *124*, 213–222. [CrossRef]
69. Dixon, L.E.; Karsai, I.; Kiss, T.; Adamski, N.M.; Liu, Z.; Ding, Y.; Allard, V.; Boden, S.A.; Griffiths, S. VERNALIZATION1 controls developmental responses of winter wheat under high ambient temperatures. *Development* **2019**, *146*, dev172684. [CrossRef] [PubMed]
70. Bernier, G.; Périlleux, C. A physiological overview of the genetics of flowering time control. *Plant Biotechnol. J.* **2005**, *3*, 3–16. [CrossRef]
71. Ejaz, M.; von Korff, M. The Genetic Control of Reproductive Development under High Ambient Temperature. *Plant Physiol.* **2016**, *173*, 294–306. [CrossRef]
72. Ochagavía, H.; Kiss, T.; Karsai, I.; Casas, A.M.; Igartua, E. Responses of Barley to High Ambient Temperature Are Modulated by Vernalization. *Front. Plant Sci.* **2022**, *12*, 776982. [CrossRef] [PubMed]
73. Zahn, T.; Zhu, Z.; Ritoff, N.; Krapf, J.; Junker, A.; Altmann, T.; Schmutzer, T.; Tüting, C.; Kastritis, P.L.; Babben, S. Novel exotic alleles of EARLY FLOWERING 3 determine plant development in barley. *J. Exp. Bot.* **2023**, *74*, 3630–3650. [CrossRef]
74. Zhu, Z.; Esche, F.; Babben, S.; Trenner, J.; Serfling, A.; Pillen, K.; Maurer, A.; Quint, M. An exotic allele of barley EARLY FLOWERING 3 contributes to developmental plasticity at elevated temperatures. *J. Exp. Bot.* **2023**, *74*, 2912–2931. [CrossRef] [PubMed]
75. Chaves, M.M.; Maroco, J.P.; Pereira, J.S. Understanding plant responses to drought—From genes to the whole plant. *Funct. Plant Biol.* **2003**, *30*, 239–264. [CrossRef] [PubMed]
76. Vaezi, B.; Bavei, V.; Shiran, B. Screening of barley genotypes for drought tolerance by agro-physiological traits in field condition. *Afr. J. Agric. Res.* **2010**, *5*, 881–892.
77. Barati, M.; Karami, Z.; Majidi, M.M.; Mirlohi, A.; Mostafavi, F.; Safari, M. Evaluation of wild barley species as possible sources of drought tolerance for arid environments. *Plant Genetic Res. Charact. Util.* **2017**, *16*, 209–217. [CrossRef]
78. Forster, B.P.; Ellis, R.P.; Moir, J.; Talamè, V.; Sanguineti, M.C.; Tuberosa, R.; This, D.; Teulat-Merah, B.; Ahmed, I.; Mariy, S.A.E.E.; et al. Genotype and phenotype associations with drought tolerance in barley tested in North Africa. *Ann. Appl. Biol.* **2004**, *144*, 157–168. [CrossRef]
79. Su, Z.; Ma, X.; Guo, H.; Sukiran, N.L.; Guo, B.; Assmann, S.M.; Ma, H. Flower development under drought stress: Morphological and transcriptomic analyses reveal acute responses and long-term acclimation in *Arabidopsis*. *Plant Cell* **2013**, *25*, 3785–3807. [CrossRef] [PubMed]
80. Gol, L.; Tomé, F.; von Korff, M. Floral transitions in wheat and barley: Interactions between photoperiod, abiotic stresses, and nutrient status. *J. Exp. Bot.* **2017**, *68*, 1399–1410. [CrossRef]
81. Yin, X.; Struik, P.C.; van Eeuwijk, F.A.; Stam, P.; Tang, J. QTL analysis and QTL-based prediction of flowering phenology in recombinant inbred lines of barley. *J. Exp. Bot.* **2005**, *56*, 967–976. [CrossRef] [PubMed]
82. Digel, B.; Tavakol, E.; Verderio, G.; Tondelli, A.; Xu, X.; Cattivelli, L.; Rossini, L.; von Korff, M. Photoperiod-H1 (Ppd-H1) Controls Leaf Size. *Plant Physiol.* **2016**, *172*, 405–415. [CrossRef] [PubMed]
83. Khahani, B.; Tavakol, E.; Shariati, J.V. Genome-wide meta-analysis on yield and yield-related QTLs in barley (*Hordeum vulgare* L.). *Mol. Breed.* **2019**, *39*, 56. [CrossRef]
84. Mikołajczak, K.; Ogrodowicz, P.; Gudyś, K.; Krystkowiak, K.; Sawikowska, A.; Frohmberg, W.; Górny, A.; Kędziora, A.; Jankowiak, J.; Józefczyk, D.; et al. Quantitative Trait Loci for Yield and Yield-Related Traits in Spring Barley Populations Derived from Crosses between European and Syrian Cultivars. *PLoS ONE* **2016**, *11*, e0155938. [CrossRef]

85. Tian, T.; Liu, Y.; Yan, H.; You, Q.; Yi, X.; Du, Z.; Xu, W.; Su, Z. agriGO v2.0: A GO analysis toolkit for the agricultural community, 2017 update. *Nucleic Acids Res.* **2017**, *45*, W122–W129. [CrossRef]
86. Glass, K.; Girvan, M. Annotation enrichment analysis: An alternative method for evaluating the functional properties of gene sets. *Sci. Rep.* **2014**, *4*, 4191. [CrossRef]
87. von Korff, M.; Léon, J.; Pillen, K. Detection of epistatic interactions between exotic alleles introgressed from wild barley (*H. vulgare* ssp. spontaneum). *Theor. Appl. Genet.* **2010**, *121*, 1455–1464. [CrossRef]
88. Kikuchi, R.; Kawahigashi, H.; Ando, T.; Tonooka, T.; Handa, H. Molecular and Functional Characterization of *PEBP* Genes in Barley Reveal the Diversification of Their Roles in Flowering. *Plant Physiol.* **2009**, *149*, 1341–1353. [CrossRef]
89. He, T.; Hill, C.B.; Angessa, T.T.; Zhang, X.-Q.; Chen, K.; Moody, D.; Telfer, P.; Westcott, S.; Li, C. Gene-set association and epistatic analyses reveal complex gene interaction networks affecting flowering time in a worldwide barley collection. *J. Exp. Bot.* **2019**, *70*, 5603–5616. [CrossRef] [PubMed]
90. Gol, L.; Haraldsson, E.B.; von Korff, M. Ppd-H1 integrates drought stress signals to control spike development and flowering time in barley. *J. Exp. Bot.* **2021**, *72*, 122–136. [CrossRef] [PubMed]
91. Roongsattham, P.; Pongtongkam, P.; Thongpan, A.; Kaveeta, L.; Harinasut, P.; Peyachoknagul, S. *Hd1*, *Hd3a*, and *Hd6* genes: Possible DNA methylation roles in photoperiod sensitive gene regulation of rice KDML 105 (*Oryza sativa* L.). *Kasetsart J. Nat. Sci.* **2006**, *40*, 462–471.
92. Habte, E.; Müller, L.M.; Shtaya, M.; Davis, S.J.; Von Korff, M. Osmotic stress at the barley root affects expression of circadian clock genes in the shoot. *Plant Cell Environ.* **2014**, *37*, 1321–1337. [CrossRef]
93. Ford, B.; Deng, W.; Clausen, J.; Oliver, S.; Boden, S.; Hemming, M.; Trevaskis, B. Barley (*Hordeum vulgare*) circadian clock genes can respond rapidly to temperature in an EARLY FLOWERING 3-dependent manner. *J. Exp. Bot.* **2016**, *67*, 5517–5528. [CrossRef] [PubMed]
94. Thiel, J.; Koppolu, R.; Trautewig, C.; Hertig, C.; Kale, S.M.; Erbe, S.; Mascher, M.; Himmelbach, A.; Rutten, T.; Esteban, E.; et al. Transcriptional landscapes of floral meristems in barley. *Sci. Adv.* **2021**, *7*, eabf0832. [CrossRef] [PubMed]
95. Wigge, P.A.; Kim, M.C.; Jaeger, K.E.; Busch, W.; Schmid, M.; Lohmann, J.U.; Weigel, D. Integration of Spatial and Temporal Information During Floral Induction in *Arabidopsis*. *Science* **2005**, *309*, 1056–1059. [CrossRef] [PubMed]
96. Finkelstein, R.R. Studies of Abscisic Acid Perception Finally Flower. *Plant Cell* **2006**, *18*, 786. [CrossRef]